DOI: 10.1070/RCR4588

Quantum chemical modelling of extraction separation of minor actinides and lanthanides: the state of the art

Yuri A.Ustynyuk,[a] Mikhail Yu.Alyapyshev,[b, c] Vasiliy A.Babain,[c] Nikolai A.Ustynyuk [d]

[a] *Department of Chemistry, M.V.Lomonosov Moscow State University*
Leninskie Gory 1, str. 3, 119991 Moscow, Russian Federation
[b] *V.G.Khlopin Radium Institute*
2 Murinsky prosp. 28, 194021 Saint Petersburg, Russian Federation
[c] *Saint Petersburg National Research University of Information Technologies, Mechanics and Optics*
Kronverksky prosp. 49, 19701 Saint Petersburg, Russian Federation
[d] *A.N.Nesmeyanov Institute of Organoelement Compounds, Russian Academy of Sciences*
ul. Vavilova 28, 119991 Moscow, Russian Federation

The review deals with the results of theoretical modelling of the structures and properties of actinide and lanthanide complexes with donor organic ligands used as selective extractants for separation of these elements in liquid high-level waste processing in the nuclear fuel cycle. The advantages and drawbacks of various types of ligands are discussed, including phosphinodithioic acids, tri- and polydentate ligands with O-donor centres, ligands based on N-heterocycles with softer N-donor centres and amides of N-heterocyclic carboxylic acids, which contain both types of donor atoms. A critical analysis of the potential of modern quantum chemistry methods in establishing structure–extraction behaviour relationships for various types of ligands is presented.
The bibliography includes 119 references.

Contents

I. Introduction 917
II. Methods for theoretical modelling of the structures and properties of lanthanide and actinide complexes: general 918
III. Complexes of phosphinodithioic acids 921
IV. Complexes of tridentate donor ligands with oxygen centres 925
V. Complexes with aminopolycarboxylic acids 928
VI. Complexes of polydentate ligands based on N-heterocycles 929
VII. Recent results 937
VIII. Conclusion 938

I. Introduction

Increasing global energy demand against the background of depletion of mineral resources makes the elaboration of novel, environmentally safe, reliable and economically admissible methods for energy production a strategic task. Solution to this task eventually governs the pace of the development of our civilization. In this connection, the role of nuclear power engineering as one of the major methods grows steadily. A key obstacle to wide use of nuclear power

Yu.A.Ustynyuk Doctor of Chemical Science, Professor of the Department of Chemistry, MSU.
Telephone: +7(495)939–2677, e-mail: ustynyuk@nmr.chem.msu.ru
Current research interests: physical chemistry, organic chemistry, supramolecular chemistry, quantum chemistry, chemistry of coordination compounds, NMR spectroscopy, chemical education.
M.Yu.Alyapyshev PhD, Deputy Director of Applied Radiochemistry Division at the KRI and Researcher at the ITMO University.
E-mail: mikkaly@gmail.com
V.A.Babain PhD, Researcher at the ITMO University, Chief Technologist at the ThreeArc Mining Ltd. E-mail: babainv@mail.ru
Current research interests of authors: extraction.
N A Ustynyuk Doctor of Chemical Science, Professor, Head of Laboratory for Organometallic Compounds at the INOC, RAS.
Telephone: +7(499)135–5064, e-mail: ustynyuk@ineos.ac.ru
Current research interests: organic chemistry, organometallic chemistry, supramolecular chemistry, chemistry of coordination compounds.

Received 15 July 2015
Translation: A.M.Raevskiy

© 2016 Russian Academy of Sciences and Turpion Ltd.

engineering consists in problems related to production of large amounts of radioactive waste. Therefore, the development of new, environmentally safe technologies of nuclear waste reprocessing and (long-term) disposal has been a challenging problem to researchers and engineers working in many countries.

At present, the main technology used for reprocessing of spent nuclear fuel (SNF) is the PUREX process (an acronym for Plutonium Uranium Recovery by Extraction). Fuel rods unloaded from a reactor after holdup time for decay of short-lived radionuclides are cut and their contents is dissolved in nitric acid. Then, uranium and plutonium are extracted (re-extracted) from aqueous nitric acid solutions into a hydrocarbon solvent using tributyl phosphate (TBP). The aqueous nitric acid solutions (PUREX raffinate) represent the bulk of high-level waste (HLW) and contain other radioactive fission products including isotopes of transuranium elements (so-called minor actinides (MA), namely, neptunium, americium and curium). The content of MA is at most 0.1% of HLW by mass, but it is these elements that are the most environmentally hazardous because of long half-lives (7370 years for Am-243, 8500 years for Cm-245, 15.6 000 000 years for Cm-247 and 348 000 years for Cm-248). In this connection, an advanced closed nuclear fuel cycle should involve, as a key step, selective extraction of MA from PUREX raffinate and their oxidation followed by transmutation to stable nuclides in a fast neutron reactor. Transmutation of MA is hampered by the presence of lanthanides having similar chemical properties and characterized by very large thermal neutron capture cross-sections. Depending on the degree of fuel burnup, the content of lanthanides in PUREX raffinate is 20–50 times higher than that of MA; this additionally complicates selective extraction of MA.

Minor actinides are separated from lanthanides by countercurrent extraction in an aqueous phase–organic phase two-phase system using organic neutral or anionic donor reactants (ligands) as extractants capable of forming strong, organic-soluble complexes with lanthanides (Ln) and actinides (An). Countercurrent extraction offers considerable advantages over other methods, being the simplest continuous process which provides high rates of mass exchange. The state of the art in the field is well documented in many monographs and reviews (see, *e.g.*, a monograph [1] and references cited therein). Modern trends in fractionation of HLW are analyzed in another review published in this issue of *Russian Chemical Reviews*.[2]

Fundamentally, the separation of actinides and lanthanides in SNF reprocessing, as well as the separation of lanthanides and actinides within each group of compounds belong to classical problems in molecular recognition of chemical systems with similar structures and properties. A modern optimum strategy for solving this class of problems is as follows. First, experimental data and theoretical considerations are used to reveal general laws and trends that govern the relationships between the recognition structure and the target property. Then, trial structures of ligands (extractants) are designed taking into account these relationships and the necessary amounts of extractants are synthesized to carry out the extraction experiments (tests) themselves. Experimental data are analyzed, the problem is refined, the extractant structures are modified and the cycle is repeated until a desired result is obtained. The contributions of experimental data and results of different-level theoretical studies depend on details that are specific to each particular task.

For long, so-called 'reasonable screening' has been the major strategy in the design of selective ligands for binding and separating lanthanides and MA. It is based on the synthesis of large series of compounds chosen based on the previous experience and on qualitative intuitive considerations and subsequent tests of these compounds. The available experience clearly shows that further progress in solving this type of problems requires a deep insight into the nature of metal–ligand bonding in the complexes of lanthanides and actinides and into the 'structure–extraction behaviour' relationships for various types of ligands. This information can be obtained by theoretical modelling of corresponding systems using different methods; among them, quantum chemistry methods are the most informative. This provides an explanation for ever-growing number of publications devoted to quantum chemical studies of the lanthanide and actinide complexes with donor ligands.

A steady increase in the contribution of the results of theoretical modelling of chemical systems using high-level quantum chemistry methods including supercomputer clusters has been a common trend particularly pronounced in the last twenty-five years. Supercomputer modelling allows one not only to hugely reduce the computational cost of calculations, but often provides a kind of information on the mechanisms of chemical reactions that cannot be obtained experimentally. Moreover, rapid progress in quantum chemistry methods and dramatic increase in performance of personal computers made it possible to calculate the structures and properties of molecular systems comprising hundreds of atoms on personal computers and to obtain reliable results that can, within the framework of particular models, be directly compared with experimental data. Methods of quantum chemical modelling have been applied to problems in extraction separation of actinides and lanthanides for prognostic purposes since quite recently. In this review we will analyze the results obtained in this field in the last fifteen years and consider prospects for utilizing these results in the development of new extraction technologies.

II. Methods for theoretical modelling of the structures and properties of lanthanide and actinide complexes: general

II.1. Quantum chemistry methods for calculating the structure and properties of lanthanide and actinide compounds

Calculations of the structures and properties of the 4f-element compounds (lanthanides) and 5f-element compounds (actinides) belong to the most difficult problems in quantum chemistry. These many-electron systems are characterized by a wealth of different-multiplicity states with close energies. Therefore, the need for correct inclusion of the electron correlation effects and relativistic effects becomes of particular importance. The nature of these effects has been considered in detail in many textbooks and monographs (see, *e.g.*, monograph [3]). The state of the art in the application of various quantum chemistry methods in relativistic calculations of lanthanide and actinide compounds and a detailed critical analysis can be found in an excellent monograph,[4] which includes a total of sixteen

chapters written by the worldwide recognized experts and in reviews.[5,6]

The accumulated experience shows that reliable results of prognostic value can be obtained only using post-Hartree–Fock methods with inclusion of electron correlation effects at a level of at least MP4(SDQ) (many-body fourth-order Möller–Plesset perturbation theory with inclusion of single, double and quadruple excitations) and (or) methods of the density functional theory (DFT) based on the generalized gradient approximation (GGA) with nonempirically constructed and hybrid functionals. The most widely used GGA-functionals are as follows: PBE,[7] PW91[8] and BP86.[9] The hybrid density functionals usually include the B3LYP[10] and PBE0.[11,12] Opinions are different as to what are the best density functionals (GGA or hybrid ones) for calculations of the actinide and lanthanide complexes. Vetere *et al.*[13,14] believe that more reliable results can be obtained using the GGA-functionals. Many other density functionals are available. Taken altogether, they form a hierarchy of DFT methods. A thorough analysis of the assumptions and scope can be found in the literature (see, *e.g.*, Refs 15–17). It is a good practice to use two or more density functionals to validate the stability of the results obtained.

The quality of a basis set used in the calculations is of paramount importance. The best results can be obtained using polarized split-valence basis sets augmented with diffuse functions [6-31G(d,p), 6-311G(3df,2p), 6-31G+(d,p), 6-311G++(3df,2p)] or correlation-consistent polarized split-valence basis sets of the type *aug*-cc-pVTZ. The potential of different approaches and methods in the calculations of actinide compounds were compared in a review by Schreckenbach and Shamov.[18]

The magnitude of direct (scalar) relativistic effects and the effects induced by the spin–orbit coupling is nearly proportional to the squared atomic number of the element (Z^2). Therefore, the description of the chemical and physical properties of compounds of the heavy elements, namely, actinides ($90 \leqslant Z \leqslant 103$) and lanthanides ($58 \leqslant Z \leqslant 71$), is impossible without correct inclusion of relativistic effects. These effects lead to stabilization (a decrease in energy) and contraction of the s-AOs and p-AOs. On the contrary, strongly shielded d-AOs and f-AOs become more diffuse and their energies increase. In the case of the lanthanide and actinide compounds, this gives rise to a wealth of different-multiplicity states with close energies. This in some extent concerns the onset of the lanthanide (actinide) contraction. Relativistic calculations are often carried out using a combination of DFT with the zeroth-order regular approximation (ZORA; here the relativistic terms appear in the one-electron integrals[19]) or with the scalar-relativistic approach proposed by Dyall.[20] The approximation using the relativistic effective core potentials (RECP) is the least computationally expensive.[21] It is based on the fact that the core electrons are usually not directly involved in chemical bonding. Therefore, their indirect influence on various properties can be described by the parameterized potential. However, the estimates of the degree of involvement of the in-core 4f- and 5f-electrons in chemical bonding obtained in this approximation should be used with care. Most methods of the relativistic post-Hartree–Fock calculations mentioned above are incorporated into modern quantum chemical software packages (PRIRODA, GAUSSIAN, MOLPRO, MOLCAS, TURBOMOL, NWCHEM, DIRAC).

II.2. Modelling of extraction equilibria and the inclusion of the effects of the medium

Both lanthanide and actinide cations can form complexes of different stoichiometry with donor ligands. The coordination number (C.N.) of the central ion in the complexes can vary from 6 to 12. Extraction involves a complex system of consecutive and concurrent equilibrium reactions in the aqueous and organic phases and at the interface between them; in most cases, information on these reactions is incomplete. An example is provided by the extraction of an M^{3+} ion from an aqueous solution containing nitric acid into a polar organic solvent using a monodentate organic anion L^- as extractant. Taking into account the fact that nitrate anions in the lanthanide and actinide complexes most often act as bidentate ligands, various hydrated complex ions and neutral complexes can co-exist in the aqueous phase. A number of equilibria involving these species are presented in Scheme 1 [equilibria (1)–(3)]. For each hydrated complex, water molecules and nitrate anions in the inner coordination sphere of the metal can be replaced by the ligands L^- in the course of the substitution reactions at the interface [see equilibria (4)–(6) in Scheme 1].

Scheme 1

$$[M(H_2O)_n]^{3+} + NO_3^- \rightleftharpoons [M(H_2O)_{n-2}(NO_3)]^{2+} + 2H_2O \quad (1)$$

$$[M(H_2O)_{n-2}(NO_3)]^{2+} + NO_3^- \rightleftharpoons \quad (2)$$

$$\rightleftharpoons [M(H_2O)_{n-4}(NO_3)_2]^+ + 2H_2O$$

$$[M(H_2O)_{n-4}(NO_3)_2]^+ + NO_3^- \rightleftharpoons \quad (3)$$

$$\rightleftharpoons [M(H_2O)_{n-6}(NO_3)_3] + 2H_2O$$

$n = 8, 9$ *etc.*

$$[M(H_2O)_{n-2}(NO_3)]^{2+} + L^- \rightleftharpoons \quad (4)$$

$$\rightleftharpoons [ML(H_2O)_{n-3}(NO_3)]^+ + H_2O$$

$$[ML(H_2O)_{n-5}(NO_3)_2] + L^- \rightleftharpoons \quad (5)$$

$$\rightleftharpoons [ML_2(H_2O)_{n-6}(NO_3)_2]^- + H_2O$$

$$[M(H_2O)_{n-6}(NO_3)_3] + L^- \rightleftharpoons [ML(H_2O)_{n-6}(NO_3)_2] + NO_3^- \quad (6)$$

$n = 8, 9$ *etc.*

$$L^- + H_3O^+ \rightleftharpoons LH + H_2O \quad (7)$$

Products, *i.e.*, $[L_mM(H_2O)_{n-m-2k}(NO_3)_k]^{(3-k)+}$ complexes ($n = 8, 9$), are transferred to the organic phase. In turn, the anionic ligand L^- undergoes reversible protonation in the acidic medium [see Scheme 1, equilibrium (7)].

The solvent extraction systems used in real experiments are even more complex because of the presence of 'alien' cations and anions that compete with the target cation M^{3+} and extractant L^-, respectively, in the equilibria. However, for many extraction systems, researchers know, from some other experimental data, the structure of the target-metal complexes that are transferred to the organic phase as well as the ratio of the hydrated complex ions present in the aqueous phase. Usually, this allows one to significantly decrease the number of the equilibrium reactions to be modelled and thus obtain a reduced but reasonably correct model for the extraction system, which includes two or three equilibria. This first step is of paramount importance. It is

the quality of the model used, other factors being equal, that governs the reliability and value of the results of theoretical modelling.

The key parameters of an extraction system, which are observed experimentally and should be modelled, include the distribution ratios (D) of the cations being extracted. They are defined as the concentration ratio of the target cation in the organic and aqueous phases.

$$D = \frac{C_{M_{(org)}}}{C_{M_{(aq)}}}$$

For extraction separation of two cations, M^1 and M^2, the separation factor (SF_{M^1/M^2}) is defined as the ratio of the distribution ratios of the cations.

$$SF_{M^1/M^2} = \frac{D_{M^1}}{D_{M^2}}$$

These quantities can be calculated with ease by quantum chemistry methods for an equilibrium using the isolated-molecule approximation corresponding to gas-phase processes. Let, *e.g.*, the reduced model for an extraction system for the separation of cations M^1 and M^2 include two equilibria described by Eqns (8) and (9).

$$[M^1(H_2O)_3(NO_3)_3] + 3\,L \overset{K_{M^1}}{\rightleftharpoons} [M^1L_3(NO_3)_3] + 3\,H_2O \quad (8)$$

$$[M^2(H_2O)_3(NO_3)_3] + 3\,L \overset{K_{M^2}}{\rightleftharpoons} [M^2L_3(NO_3)_3] + 3\,H_2O \quad (9)$$

The equilibrium constants (K_{M^1} and K_{M^2}) can be determined using expression (10) upon calculating the Gibbs energies of these equilibria (ΔG_{M^1} and ΔG_{M^2}) that are equal to the Gibbs energy differences between the starting compounds and final products.

$$K_M = \exp\left(-\frac{\Delta G_M}{RT}\right) \quad (10)$$

Then, the separation factor of the process is given by expression (11) where $\Delta\Delta G_{M^{1,2}}$ is a simple Gibbs energy difference between two equilibria [Eqn. (12)].

$$SF_{M^1/M^2} = \frac{K_{M^1}}{K_{M^2}} = \exp\left(-\frac{\Delta\Delta G_{M^{1,2}}}{RT}\right) \quad (11)$$

$$\Delta\Delta G_{M^{1,2}} = \Delta G_{M1} - \Delta G_{M^2} \quad (12)$$

Usually, it is assumed that complexes of cations with organic ligands are completely transferred to the organic phase. In this case, the equilibrium constants K_{M^1} and K_{M^2} are linearly related to the distribution ratios D and the ratio of the equilibrium constants equals the separation factor of the process, SF_{M^1/M^2}. This makes it possible to compare the results of calculations with experimental data and thus assess the quality of the model and calculations.

Since the processes under study occur in the aqueous and organic phases and at the interface between them, phenomena usually called the effects of the medium (*i.e.*, the ability of ligands to undergo protonation, as well as solvation of metal cations and complexes in both phases and hydrogen bonding resulting in the formation of the second coordination sphere of the complexes) should undoubtedly influence the distribution ratios and the An/Ln separation factors. Experimental data show that this does occur and the effect may be strong. Therefore, modelling of extraction equilibria requires carrying out quantum chemical calculations with inclusion of the effects of the medium; this is a specific complicated problem. Methods for solving this problem have been considered in a number of monographs and reviews (see, *e.g.*, review [22]).

There are two types of commonly used models for the description of solvation effects. These are the continuum models and the cluster ones. The former treat a solvent as isotropic polarizable dielectric continuum characterized by the dielectric constant ε (PCM model,[23,24]) or as conductor (COSMO model,[25,26]) and ignore specific solute–solvent interactions, such as hydrogen bonding or the formation of donor–acceptor complexes. In the latter case, the solute molecule and the solvent molecules forming its first (in some cases, the second) coordination sphere are treated as a supermolecule. This type of models is free from the drawback mentioned above, although there are some uncertainties due to *a priori* unknown number of solvent molecules that should be included in the supermolecule to obtain a correct description of the system in question. It is believed that the situation can be clarified using two approaches. One of them is to apply a continuum model to the supermolecule (solute molecule and solvent molecules in the first coordination sphere). The other uses the QM/MM methods, namely, the supermolecule is calculated rather accurately by the quantum mechanical (QM) method while the environment (solvent molecules in the second and third coordination spheres) is described by the molecular mechanics (MM) methods. Examples of successful application of the second approach to elucidate the structures of the aqua complexes of lanthanides and actinides in aqueous solutions can be found in the literature [26–32] (see†). Studies on the extraction separation of actinides and lanthanides reported so far have been carried out with inclusion of solvation effects using the continuum models only.

II.3. The principle of hard and soft acids and bases

The extraction properties of different-type ligands for the separation of lanthanides and actinides are often qualitatively considered in terms of Pearson's acid base concept, or the hard and soft acids and bases (HSAB) concept. Following this concept, both Ln^{3+} and An^{3+} cations, which have small ionic radii and bear high charges, are treated as hard Lewis acids. The absolute hardness of an acceptor (η) can be assessed using expression (13)

$$\eta = \frac{I - A}{2} \quad (13)$$

where I is the first ionization potential and A is the electron affinity. In the case of organic compounds, I is taken equal to $-E_{HOMO}$ while A is taken equal to $-E_{LUMO}$. The reference pair for estimating the selectivity of ligands in the separation of lanthanides and actinides includes the Eu^{3+} and Am^{3+} cations. Their ionization potentials and electron affinities are listed in Table 1.

† A Correction to Ref. 30 is available. See G A Shamov, G Schreckenbach *J. Phys. Chem. A* **110** 12072 (2006).

Table 1. Ionization potentials, electron affinities and absolute hardnesses of Eu^{3+} and Am^{3+} cations.

Cation	I/eV	A/eV	η
Eu^{3+}	−37.16	−31.95	2.60
Am^{3+}	−32.40	−28.45	1.97

From the data of Table 1 it follows that the much softer Am^{3+} cation and other An^{3+} cations should exhibit higher affinity for ligands with soft donor centres compared to Ln^{3+} cations. This simple qualitative concept is basic to the search for selective ligands for the extraction separation of actinides and lanthanides in the early steps of research. Indeed, both actinide and lanthanide cations exhibit very high affinity for hard Lewis bases with oxygen donor centres, but this type of bases usually exhibits no high selectivity. In this connection, ligands containing somewhat softer donor S- and N-centres have attracted increasingly greater attention in the design of new extractants.

Researchers from China reported a review[33] of studies on quantum chemical modelling of lanthanide and actinide complexes formed in the course of extraction separation of these elements carried out before 2010. In the text below these studies will be touched upon only to the extent necessary to understand the results obtained more recently.

III. Complexes of phosphinodithioic acids

A number of publications on theoretical modelling of complexes of dialkylphosphinodithioic acids $R_2P(S)SH$ with lanthanides and actinides are available.[34–43] These ligands exhibit very high separation factors in the extraction separation of lanthanides and MA. In 1996, Zhu *et al.*[34] showed that bis(2,4,4-trimethylpentyl)phosphinodithioic acid (Cyanex-301, Fig. 1) provides a separation factor, $SF_{Eu/Am}$, of 5900. Another group of researchers from China reported that changes in the structure of the alkyl substituent in this compound have little effect on the $SF_{Eu/Am}$ values.[35] For instance, dialkylphosphinodithioic acids with isomeric alkyl fragments C_8 (n-octyl, 1-methylheptyl, 2-ethylhexyl) are characterized by the following $SF_{Eu/Am}$ values: 9.7×10^3, 1.0×10^4 and 1.0×10^4, respectively.

The stoichiometry and structure of the lanthanide and actinide complexes with thiophosphinic acids depend on various factors. Among them, the most important are the ionic radius of the central ion and the volume of the ligands. Boland *et al.*[36] studied reactions of anhydrous cerium, neodymium, samarium, gadolinium and ytterbium chlorides with sodium phosphinodithioate in organic solvents and showed that lanthanides with large ionic radii (Ce^{3+}, Nd^{3+}, Sm^{3+}, Eu^{3+}) form anionic complexes $[Ln(S_2PPh_2)_4]^-$ with this ligand. In all cases, phosphinodithioate anions act as bidentate ligands, while the central metal atoms form eight coordination bonds with sulfur atoms. Lanthanides with smaller ionic radii, Gd and Dy, form a mixture of complexes. Among them, both anionic complexes $[Et_4N]^+[Ln(S_2PPh_2)_4]^-$ (Ln = Eu, **1**) and neutral complexes $[Gd(S_2PPh_2)_3(NCMe)_2]$ and $[Dy(S_2PPh_2)_3(NCMe)_2]$ (**2**) (Fig. 2) were isolated and structurally characterized. In these species, one anionic ligand is replaced by two acetonitrile molecules (acetonitrile was used as solvent in the reaction). Eventually, ytterbium, which has the smallest ionic radius among all elements studied, forms an anionic complex $[Ph_4P]^+[Yb(S_2PPh_2)_3Cl]^-$ (**3**); here, the coordination number of the metal ion decreases to 7 and one position is occupied by chloride anion (see Fig. 2).

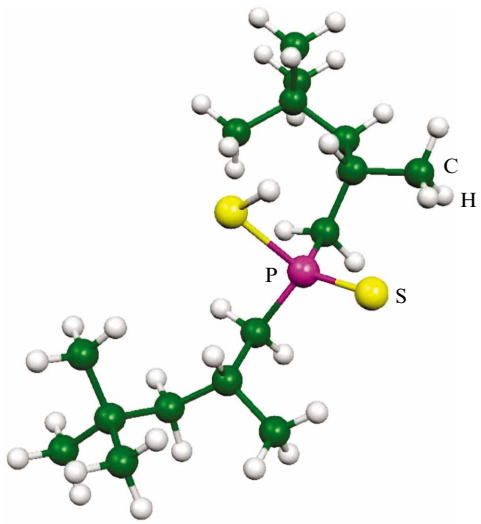


Figure 1. Optimized molecular structure of bis(2,4,4-trimethylpentyl)phosphinodithioic acid (Cyanex-301) obtained from gas-phase quantum chemical calculations.[41]

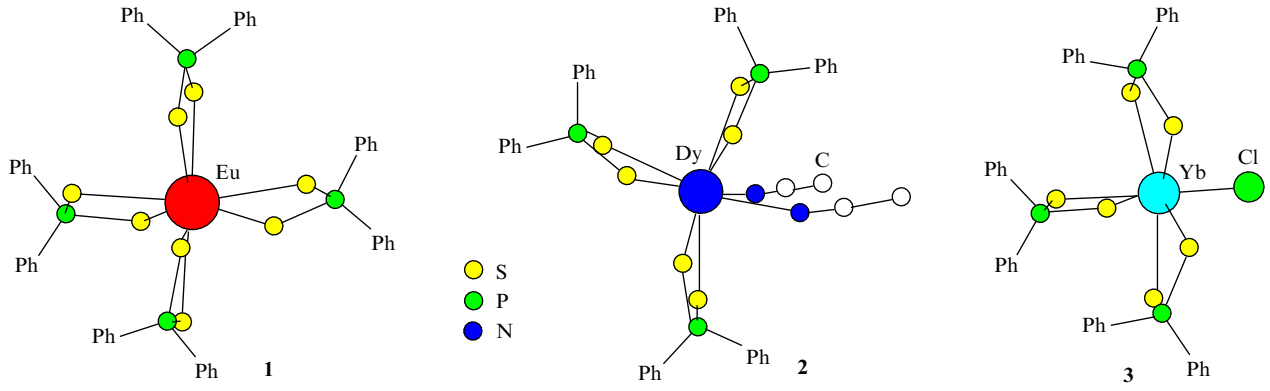


Figure 2. Structures of lanthanide diphenylphosphinodithioate complexes (see text).[36]

Reactions of lanthanide and actinide cations with dialkylphosphinodithioic acids in acidic aqueous solutions result in complexes of different composition; in particular, $[M(S_2PR_2)_3]$ and $[HM(S_2PR_2)_4]$ (M = Ln, An) can be extracted to the organic phase. Theoretical investigation of these complexes and their analogues with selenium-containing ligands have been a subject of publications.[31, 36–43] The research efforts were aimed to reveal the nature of high selectivity of dialkylphosphinodithioic acids for actinides.

Researchers from India carried out a thorough study on solvent extraction of La^{3+}, Eu^{3+}, Lu^{3+} and Am^{3+} from aqueous solutions containing nitric acid with bis(2,4,4-trimethylpentyl)phosphinodithioic acid (Cyanex-301, L) to toluene (organic phase) at different extractant/cation concentration ratios and at different pH values.[43] The solvent extraction experiments revealed that, irrespective of the extractant concentration, americium and lutetium are extracted as complexes of the type $[AmL_3]$ and $[LuL_2(NO_3)]$, respectively. Europium and lanthanum form extractable species of the type $[LnL_2(NO_3)]$ (Ln = Eu, La) at low concentrations of the ligand L (0.1 mol litre^{-1}) and of the type $[LnL_3]$ at higher L concentrations (0.5 mol litre^{-1}).

Theoretical modelling of extraction was performed[43] taking model complexes with dimethylphosphinodithioic acid $Me_2P(S)SH$ (L′) as examples. The ligand L′ was used as model for Cyanex-301 in order to reduce the computational cost. Density functional calculations were carried out using four GGA functionals (BP86, PBE, BLYP, PW91) and the polarized split-valence basis sets of the *aug*-cc-pVTZ quality. The basis sets were augmented with 4f-AOs for lanthanides and 5f-AOs for actinides, the relativistic effects were included in the ZORA approximation, and the solvent effects were considered using the COSMO continuum model. Four types of complexes, that is, $[M(NO_3)_3]$, $[ML'(NO_3)_2]$, $[ML'_2(NO_3)]$ and $[ML'_3]$ (Fig. 3) were calculated for each metal. The results obtained using different functionals appeared to be consistent. All main trends and features were reproduced correctly.

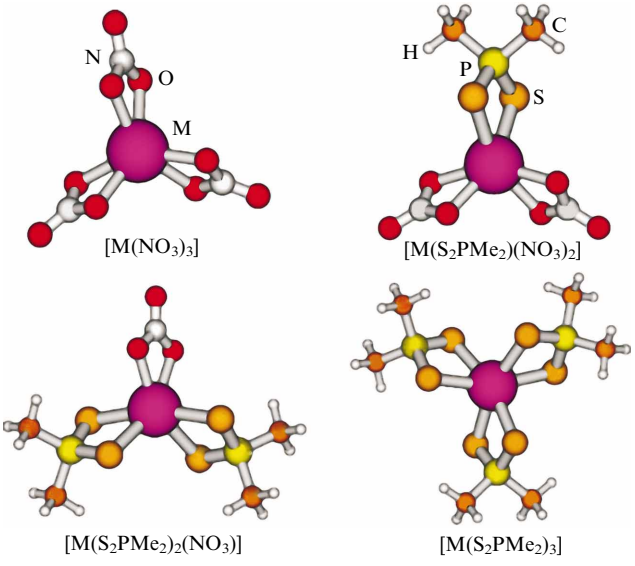


Figure 3. Types of computationally studied complexes of La^{3+}, Eu^{3+}, Lu^{3+} and Am^{3+} (see Ref. 43).

The calculated M–S, P–S and M–O bond lengths agree with the available experimental data and with the results obtained in other theoretical studies. Besides, complexation causes elongation of P–S bonds, thus indicating a decrease in their π-character owing to partial transfer of the electron density to the metal. The M–S bond lengths increase on going from the complexes $[ML'(NO_3)_2]$ to $[ML'_3]$, but in all types of complexes the Am–S bonds are much shorter than the Eu–S bonds, although the ionic radius of Am^{3+} is larger than that of Eu^{3+} (1.115 *vs.* 1.087 Å, respectively). The positive partial Mulliken atomic charges of metals in the Am^{3+} complexes are much smaller than in the Eu^{3+} complexes. The authors cited[43] believe that this is indicative of higher covalency of the Am–S bonds compared to the Eu–S bonds. The results of calculations of the Eu^{3+} and Am^{3+} complexes with the simplest S-donor ligand HS^- revealed the same trends in changes in the bond lengths and atomic charges, but the differences in the M–S bond lengths were much smaller than in the complexes with L′. It follows that steric effects that are much more pronounced for L′ should also be taken into account.

The most interesting results were obtained in calculations of the complexation energies of La^{3+}, Eu^{3+}, Lu^{3+} and Am^{3+} with L′ for the gas phase (isolated molecules) and with inclusion of solvation effects. The gas-phase complexation energies were obtained for reaction (14).

$$M(NO_3)_3 + n\,Me_2PS_2^- \rightleftharpoons [M(S_2PMe_2)_n(NO_3)_{3-n}] + n\,NO_3^- \qquad (14)$$

$n = 1–3$

These energies were calculated as the total energy differences between the starting anhydrous nitrates and corresponding complexes. The energies of the Am complexes appeared to be appreciably higher than those of the complexes of the three lanthanides. Considering the species $[ML'(NO_3)_2]$, $[ML'_2(NO_3)]$ and $[ML'_3]$, one has −4.4, −9.8 and 79.8 kcal mol^{-1} for M = Am and −5.4, 77.3 and −6.7 kcal mol^{-1} for M = Eu. These values were obtained from calculations with the BP86 functional, but calculations with other functionals gave similar results. Equal complexation energies of the complexes $[ML'_2(NO_3)]$ and $[ML'_3]$ for M = Am and even lower complexation energy of $[ML'_3]$ for M = Eu are in good agreement with the experimental fact that for these two metals the type of the complex being extracted depends on the cation/ligand concentration ratio. Higher complexation energies of Am excellently reproduce high selectivity of phosphinodithioic acids for americium observed in the extraction experiments.

The effects of solvent were included[43] within the framework of the COSMO approach. The most interesting information was obtained from the 'extraction energies' calculated using Eqn (15).

$$M^{3+}_{(aq)} + n\,Me_2PS^-_{2\,(tol)} + (3-n)\,NO^-_{3\,(aq)} \rightleftharpoons \qquad (15)$$

$$\rightleftharpoons [M(S_2PMe_2)_n(NO_3)_{3-n}]_{(tol)}$$

It was found that for M = Am the extraction energies of the complexes $[ML'_2(NO_3)]$ and $[ML'_3]$ (−7.8 and −9.5 kcal mol^{-1}, respectively) are higher in absolute value than those of the complexes with M = Eu (−3.5 and −4.6 kcal mol^{-1}, respectively). This result also makes it clear that phosphinodithioic acids exhibit much higher affinity for americium,

being in excellent agreement with experimental data. Undoubtedly, an important contribution comes from the higher dehydration energy of Eu^{3+} ions compared to Am^{3+} ions {in aqueous solutions, both ions exist as the aqua complexes $[M(H_2O)_n]^{3+}$ (M = Am, Eu; n = 8, 9)}. Therefore, high selectivity of phosphinodithioic acids as ligands for the extraction of actinides and lanthanides is due to two complementary factors, namely, higher covalency of Am–S bonds compared to Eu–S bonds and higher dehydration energy of Eu^{3+} ions compared to that of Am^{3+} ions when water molecules are displaced by the ligand.

Recognizing high quality of the study by Bhattacharyya *et al.*,[43] two important remarks should be made. The models used do not directly include the role of water molecules and the acidity of the medium. This drawback was also pointed out by the authors of that publication. In particular, representation of weak acid $Me_2P(S)SH$ by the anion $Me_2P(S)S^-$ in acidic media is manifestly unjust. Besides, much higher 'extraction energies' of the lutetium complexes $[LuL'_2(NO_3)]$ and $[LuL'_3]$ (−7.2 and −6.0 kcal mol^{-1}) have no explanation within the framework of the models used. Eventually, discussing positions of chemical equilibria requires calculations of the Gibbs energies ΔG, which can vary over a wide range when long branched alkyl substituents are replaced by methyl groups.

High selectivity of bis(2,4,4-trimethylpentyl)phosphinodithioic acid (Cyanex-301, L) for americium was also studied by researchers from Germany.[41] The structures of the ligand and its complexes of the types $[ML_3]$ and $[HML_4]$ (M = Am, Cm, Eu) were calculated without structural simplifications. The calculated structures of the $[ML_3]$ complexes have a C_3 symmetry (Fig. 4). Most calculations were carried out by the DFT/BP86 method with two extended split-valence basis sets, def2-TZVP and QZVP. Relativistic effects were described using the relativistic, energy-consistent, ab initio 4f-in-core pseudopotentials for europium and 5f-in-core pseudopotentials for actinides. Additional energy calculations for a number of structures with DFT-optimized geometries were carried out within the framework of the many-body MP2 perturbation theory for calibration purposes.

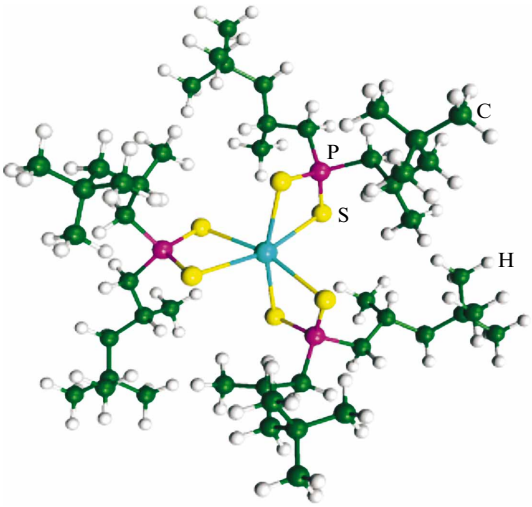


Figure 4. Calculated structure of complexes $[ML_3]$ [M = Am, Cm, Eu; L = $R_2PS_2^-$, R = bis(2,4,4-trimethylpentyl)].[41]

It was shown that cations are most probably extracted as complexes of the type $[ML_3]$ (M = Am, Cm, Eu). In this connection, equilibrium (16) was simulated.

$$M^{3+} + 3\,HL \rightleftharpoons [ML_3] + 3\,H^+ \qquad (16)$$

M = Am, Cm, Eu

Geometry optimization of the complexes was performed for the gas-phase conditions. The Gibbs energies of the gas-phase equilibria (ΔG_g) were calculated as the Gibbs energy differences between the starting compounds and products following Eqn (17).

$$\Delta G_g = G_g([ML_3]) + 3\,G_g(H^+) - G_g(M^{3+}) - 3\,G_g(HL) \qquad (17)$$

Since the metal ions (M^{3+}) and protons (H^+) are in the aqueous phase, while the ligand L and complexes $[ML_3]$ reside in the organic phase (hydrocarbon solvent), the changes in the Gibbs energies in solution (ΔG_{solv}) were determined using expression (18). The corrections, $\Delta\Delta G_{solv}$, are given by Eqn (19).

$$\Delta G_{solv} = \Delta G_g + \Delta\Delta G_{solv} \qquad (18)$$

$$\Delta\Delta G_{solv} = G_{solv}([ML_3]) + 3\,G_{aq}(H^+) - G_{aq}(M^{3+}) - 3\,G_{solv}(HL) \qquad (19)$$

The solvation effects ΔG_{solv} were included in a combined fashion. The hydration energy of H^+ was assumed to be equal to the experimental value, *viz.*, −264.2 kcal mol^{-1}.[44] The experimental hydration energy of Eu^{3+} is −804.8 kcal mol^{-1}.[45] However, here we used the results of the DFT calculations by Dolg and co-workers,[31] namely, −754.1 kcal mol^{-1} for Eu^{3+} and −716.3 kcal mol^{-1} for Am^{3+} as the corresponding ΔG_{solv} values (emphasize that both values were calculated by the same method). The hydration energies of the ligand L and complexes $[ML_3]$ were determined within the framework of the COSMO model.

The results obtained by Cao *et al.*[41] are significantly different from those reported by researchers from India.[43] The M–S bond lengths in the complexes $[ML_3]$ are larger than in the complexes $[ML'_3]$, probably due to noticeable influence of the steric strain produced by the long branched hydrocarbon groups in the first coordination sphere of metals in the complexes $[ML_3]$. The elongation is most pronounced for $[AmL_3]$ (0.08 Å). According to calculations, the Am–S bond is 0.055 Å shorter than the Eu–S bond, the difference being larger than the ionic radii difference between americium and europium (0.028 Å). The positive atomic charge of Am in the complex $[AmL_3]$ is higher than that of Eu in the complex $[EuL_3]$ (+1.21 *vs.* +0.94, respectively); this also holds for the averaged negative atomic charges of sulfur (−0.455 and −0.435 in the Am and Eu complexes, respectively). It follows that Am–S bonds are more ionic in character than Eu–S bonds. An analysis of orbital populations showed that f-AOs are only slightly involved in chemica bonding.

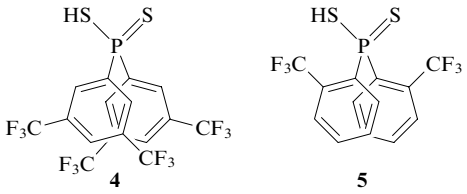
Gas-phase complexation resulting in $[EuL_3]$ and $[AmL_3]$ (see Eqn. (16)) is an endothermic process (ΔG_g = 15.26 kcal mol^{-1} for $[EuL_3]$ and 34.23 kcal mol^{-1} for $[AmL_3]$). The

europium complex is much more stable in the isolated-molecule approximation; this contradicts the results obtained in the extraction experiments. However, the situation is reversed, *i.e.*, complexation becomes exothermic (this agrees with experimental data) when the effects of the medium are included using the COSMO approach (see above). The energy gain ΔG_{solv} for $[AmL_3]$ (-80 kcal mol^{-1}) is much higher than for $[EuL_3]$ (-12.95 kcal mol^{-1}). Thus, calculations predict that the europium complex is much less stable than the americium complex in the two-phase system under study; this is immediately related to the higher desolvation energy of Eu^{3+} ion in water. It is this contribution that is responsible for high selectivity of dialkylphosphinodithioic acids for americium in the extraction experiments.[41]

Cao *et al.*[41] made a critical analysis of their results and pointed out a number of uncertainties. Firs of all, this concerns imperfection of the chemical model used, which ignores the fact that americium and europium ions are present in aqueous solutions in the form of octa- and nonahydrates $[M(H_2O)_n]^{3+}$ ($n = 8, 9$), additionally solvated by water molecules that form the second coordination sphere through hydrogen bonds. These specific interactions are ignored by the continuum models for solvation. It is also unclear how the inclusion of f-AOs in the core pseudopotentials may influence the results of calculations. Conclusion drawn by the authors[41] contradict not only those made by many other researchers, but also almost commonly accepted point of view, according to which higher thermodynamic stability of actinide complexes arises from higher covalency of An–X bonds compared to Ln–X bonds. Therefore, Dolg *et al.*[46] carried out an additional quantum chemical study of $[EuL_3]$ and $[AmL_3]$ complexes. The structures and energies of these species were obtained from DFT calculations with different functionals and f-in-valence ('small-core') pseudopotentials, as well as from unrestricted Hartree–Fock and MP2 calculations. Most DFT calculations gave conventional results, namely, the calculated Am–S interatomic distances are shorter than the Eu–S interatomic distances irrespective of the type of the functional and pseudopotential. However, the MP2 and unrestricted Hartree–Fock calculations with better inclusion of electron correlation effects led to different results, *viz.*, the Am–S bonds are longer than Eu–S ones in agreement with the ionic radii of the elements. Since more rigorous calculations of the large systems modelling the $[ML_3]$ complexes were not feasible, simpler model compounds were used. These were americium and europium iodides MI_3 where the lanthanide and actinide atoms form bonds with soft donors. The experimentally determined Eu–I bond length in EuI_3 is 2.831 ± 0.022 Å. This value is reproduced with a reasonable accuracy in the most reliable CCSD(T) coupled cluster calculations (2.841 Å) and in the MP2 calculations (2.822 Å). Calculations of the Am–I bond length in AmI_3 by these two methods give 2.882 and 2.862 Å, respectively, which is in agreement with the ionic radii. However, DFT calculations with different functionals in all cases predict that the Am–I bond is 0.04–0.06 Å shorter than the Eu–I bond. The calculated Eu–I bond length is 0.1–0.13 Å longer than the experimental value. The authors emphasized that the bond lengths obtained from DFT calculations of lanthanide and actinide compounds are inappropriate for being a criterion for covalency, although agree that covalency can contribute to high selectivity of dialkylphosphinodithioic acids for americium in the extraction experiments. Uncertainties in DFT calculations may result from the so-called 'delocalization error', as was pointed by Cohen *et al.*[17] Noteworthy is the following. Dolg and co-workers[46] found that the results of DFT calculations of the geometry and energies using the f-in-core ('large-core') pseudopotentials are closer to the experimental values and to the results obtained by more rigorous methods. In order to eliminate the second drawback of their model and to provide a better description of the effects of hydration, Dolg and co-workers[47,48] carried out two studies on the hydration of lanthanides and actinides.

Significantly different interpretations of the results of DFT calculations in studies of the nature of selectivity of the extractants in the extraction separation of actinides and lanthanides do not exclude the possibility to use these results in practice in order to predict the extraction properties of ligands. Although dialkylphosphinodithioic acid derivatives have not been subject to prognostic investigations in the strict sense where prediction of important results is followed by experimental substantiation, the ability of DFT calculations to reproduce the observed relationships *a posteriori* was confirmed repeatedly. An example is provided by a study by Keith and Batista.[49] Indeed, Klaehn *et al.*[50] unexpectedly found that two structurally similar diarylphosphinodithioic acids used as ligands for extraction separation of americium and europium exhibit dramatically different selectivities, namely, one has $SF_{Am/Eu} \approx 20$ for bis[3,5-di(trifluoromethyl)phenyl]phosphinodithioic acid (**4**) and $SF_{Am/Eu} \approx 10^5$ for bis[2-(trifluoromethyl)phenyl]phosphinodithioic acid (**5**) (Table 2). The reasons for so large differences were examined in a DFT quantum chemical study.[49]

Structures 4, 5



4 **5**

It was assumed that complexation and extraction are described by Eqn (20) and the thermodynamic cycle shown in Fig. 5.

$$M^{3+}_{(aq)} + 3\,HL^{n}_{(org)} \rightleftharpoons [ML^{n}_{3}]_{(org)} + 3\,H^{+}_{(aq)} \qquad (20)$$

Density functional calculations were carried out with the B3LYP hybrid functional, a DZ extended split-valence basis set and relativistic pseudopotentials for Am and Eu. According to gas-phase calculations, the process described by Eqn (14) is exothermic ($\Delta G < 0$). For both ligands **4** and **5**, the ligand–Eu^{3+} binding energies appeared to be much

Table 2. Selectivity in extraction separation of Am^{3+} and Eu^{3+} using ligands **4** and **5**.[49]

Ligand	$SF_{Am/Eu}$	$\Delta\Delta G_{extr}$ /kcal mol^{-1}	$\Delta\Delta\Delta G$ /kcal mol^{-1}
4	20	-1.8	-5.0
5	100 000	-6.8	

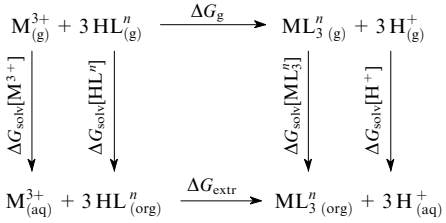


Figure 5. Thermodynamic cycle for actinide and lanthanide extraction by diarylphosphinodithioic acids **4** and **5**.[49]

higher (by 13–15 kcal mol^{-1}) than the ligand–Am^{3+} binding energies, which contradicts experimental data.

The solvation energy of a proton was assumed to be equal to the experimental value (264.2 kcal mol^{-1}), like in Ref 44, while the solvation energies of Eu^{3+} and Am^{3+} ions were estimated using the combined approach by Dolg (see above) and a semiempirical approach by David and Vokhmin.[51] Both methods led to qualitatively similar results. According to calculations with inclusion of solvation effects, the Am complexes with both ligands **4** and **5** in the two-phase system appear to be thermodynamically more favourable than the Eu complexes; this agrees with experimental data.

$$AmL^{1}_{(org)} + EuL^{2}_{(org)} \rightleftharpoons AmL^{2}_{(org)} + EuL^{1}_{(org)} \qquad (21)$$

In accordance with the thermodynamic cycle (see Fig. 5, the Gibbs energy difference $\Delta\Delta G$ observed for the equilibrium (21), which describes the separation factor difference between ligands **4** and **5**, is independent of the method for calculating the hydration energies of the americium and europium ions. The computed $\Delta\Delta G$ value is -3.09 kcal mol^{-1}, being close to a value of -5.0 kcal mol^{-1} determined using experimental data taken from Ref. 50. 'Chemical' reasons for the giant selectivity difference between two ligands with very similar structures remain unclear. Most probably, steric interaction between the bulk CF_3 groups in *ortho*-positions of phenyl rings and the sulfur atoms causes significant changes in the geometry of the coordination site, but detailed description of the molecular geometry of the complexes was not reported. We believe one should not hope for good agreement with experimental data in studies of other complex molecular systems. In the case in point, this agreement can be a result of mutual cancellaltion of errors. But even a qualitatively correct result 'with accuracy up to a sign of the effect' seems to be encouraging.

Among other studies on the nature of the metal–ligand bonding in the actinide and lanthanide complexes with S-donor ligands, mention should be made of a comparative DFT study of tris(dithiolene) complexes with uranium(III,IV) and neptunium(III) carried oust using the BP86 functional, the TZ2p basis set and the ZORA approximation.[40] A dianionic ligand 5,6-dihydro-1,4-dithiin-2,3-dithiolate (dddt) forms various complexes with transition metals, actinides and lanthanides; many of them were isolated and characterized by X-ray diffraction analysis. Figure 6 presents the calculated structures of the complex anion of neodymium (structural data for this species are shown in parentheses) and a hypothetical complex anion of trivalent uranium. The metal atoms in these complexes have a coordination number of 7. A detailed analysis of the electronic structures and orbital populations in the complexes of both anions revealed that the uranium complex is characterized by not only ligand-to-metal electron density transfer, but also π-backdonation (dative interaction), *i.e.*, partial transfer of the electron density from the metal to the π*-MO of the double bond.

IV. Complexes of tridentate donor ligands with oxygen centres

Although dialkyl- and diarylphosphinodithioic acids used as extractants exhibit excellent separation factors in the separation of lanthanides and MA, they also have a number of clearly seen disadvantages. These are (i) the possibility to achieve high distribution ratios (D) only for extraction from weakly acidic solutions, (ii) low oxidation stability and (iii) formation of solid phosphate and sulfate residues upon incineration of the complexes (this is exceptionally undesirable because of subsequent cracking of matrices on vitrification). Consequently, these ligands are inappropriate for real technological applications. Extractants containing only C, H, O and N atoms are free from this drawback and offer undoubtful advantages from the technological point of view. These compounds include one of the most promising classes, namely, diglycolic acid diamides (diglycolamides) **6**. There is considerable literature on theoretical modelling of the complexes of these ligands with lanthanides and acti-

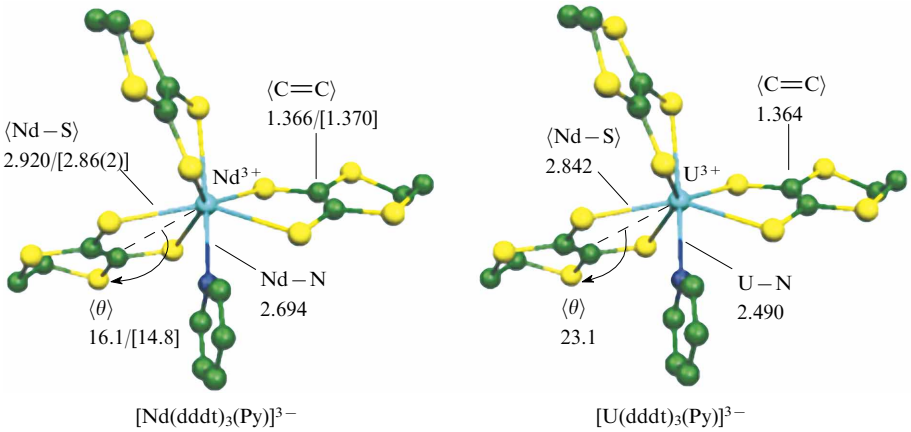
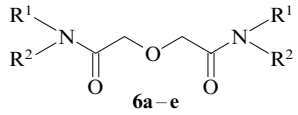


Figure 6. Structures of $[M(dddt)_3Py]^{3-}$ (M = Nd, U) anions obtained from DFT calculations.[40] Experimental geometric parameters of $[Nd(dddt)_3Py]$[37] determined by X-ray diffraction are shown in square brackets. Distances are given in Å and angles are given in degrees; Py stands for pyridine.

Structures 6



6a–e

$R^1 = R^2$ = Me (**a**), Et (**b**, TEDGA), Pr^n (**c**), n-C_8H_{17} (**d**, TODGA), R^1 = Me, R^2 = n-C_7H_{15} (**e**, DMDHOPDA)

nides.[52–69] Diamides **6a–c** with short alkyl substituents at nitrogen atoms are well soluble in water. Diamides **6d**,**e** with long alkyl chains at nitrogen atoms are very well soluble in nonpolar organic solvents and can be used as extractants. Numerous experimental studies on these ligands are reflected in a review.[52] A few theoretical studies[55–58] on the topic have been reported recently.

Depending on extraction conditions, diglycolic acid diamides can form complexes of different stoichiometry and composition with actinides and lanthanides. For instance, extraction with *N*,*N*,*N*′,*N*′-tetraoctyl diglycolamide (TODGA, **6d**) to a nonpolar (n-dodecane) or low-polarity solvent (toluene) mainly results in the 1 : 3 or 1 : 4 complexes.[59,60] Extraction to more polar 1,2-dichloroethane or octanol affords the 1 : 2 complexes, while the 1 : 1, 1 : 2 and 1 : 3 complexes co-exist in aqueous ethanol.[61] In these complexes, diglycolamides act as tridentate ligands coordinated to the metal through two carbonyl groups and the ether oxygen atom. The bonds with the carbonyl oxygen atoms are much shorter and stronger than with the ether oxygen atom.[54]

Researchers from China carried out[53] a detailed theoretical DFT study of the complexes of europium, americium and curium with two ligands, TODGA (**6d**) and *N*,*N*′-diheptyl-*N*,*N*′-dimethyl-3-oxapentanediamide (DMDHOPDA, **6e**), using the BP86 and B3LYP functionals, relativistic f-in-core pseudopotentials and the 6-31G(d) basis set; the effects of solvation were included using the COSMO approach. Full geometry optimization of the octa- and nonahydrates $[M(H_2O)_n]^{3+}$ (n = 8, 9), aqua ions $[M(NO_3)(H_2O)_7]^{2+}$, $[M(NO_3)_2(H_2O)_5]^{+}$, $[M(NO_3)_3(H_2O)_3]$, as well as complexes $[ML]^{3+}$, $[ML_2]^{3+}$, $[ML(H_2O)_6]^{3+}$, $[ML(NO_3)(H_2O)_4]^{2+}$, $[ML(NO_3)_2(H_2O)_2]^{+}$, $[ML(NO_3)_3]$ and $[ML_2(NO_3)_3]$ (M = Eu, Am; L = **6d**,**e**) was performed. As examples, Fig. 7 presents the structures of the complexes $[M(\mathbf{6d})(NO_3)_3]$ and $[M(\mathbf{6d})_2(NO_3)_3]$.

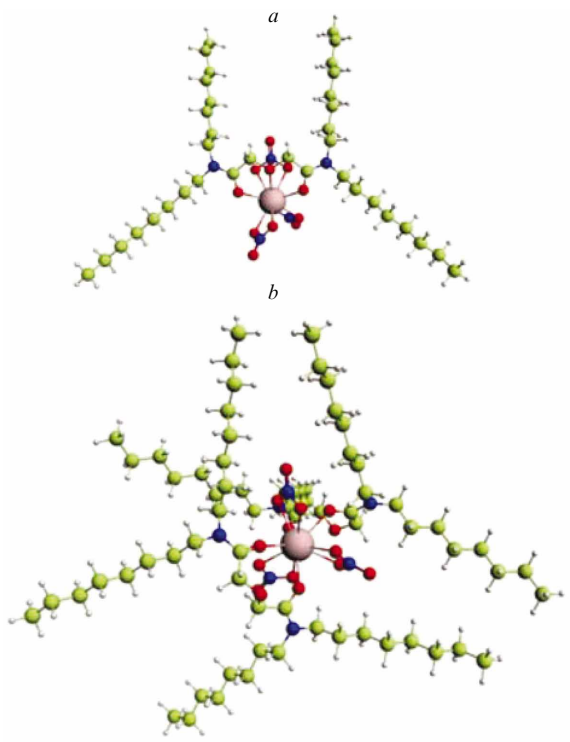


Figure 7. Structures of complexes $[M(\mathbf{6d})(NO_3)_3]$ (*a*) and $[M(\mathbf{6d})_2(NO_3)_3]$ (*b*) obtained from gas-phase DFT calculations.[53]

According to gas-phase calculations, neutral complexes $[ML(NO_3)_3]$ are the most stable species. Gas-phase thermodynamic parameters were calculated for complexation and extraction described by Eqns (22) and (23), respectively.

$$[M(H_2O)_9]^{3+} + L + 3\,NO_3^- \rightleftharpoons [ML(NO_3)_3] + 9\,H_2O \qquad (22)$$

$$[M(H_2O)_9]^{3+}_{(aq)} + L_{(org)} + 3\,NO^-_{3\,(aq)} \rightleftharpoons \rightleftharpoons [ML(NO_3)_3]_{(org)} + 9\,H_2O_{(aq)} \qquad (23)$$

The nature of the metal–oxygen coordination bonds in the complexes was examined using the natural bonding orbital (NBO) approach, which involves transformation of delocalized many-electron wavefunctions to the natural orbitals that describe the electronic structure of a molecular system in terms of localized bonding and nonbonding orbitals.[62] The calculated Wiberg indices of the M ← O bonds lie in the range from 0.10 to 0.37 and correspond to a noticeable covalency of these bonds, the covalent contribution being larger for the metal–carbonyl oxygen bonds. From the populations analysis it follows that negative charges on the carbonyl oxygen atoms are larger than on the ether oxygens and there is considerable transfer of the electron density from the ligand oxygen atoms to the metal. The degree of charge transfer is higher for the europium complexes, which are more thermodynamically stable in the gas phase. However, the situation is reversed upon the inclusion of solvent effects [Eqn (23)]. The thermodynamic characteristics of the extraction processes are listed in Table 3.

The results of calculations agree with experimental data, namely, both ligands **6d** and **6e** are expected to exhibit higher selectivity for americium, the selectivity being more pronounced for **6e**. For both the gas phase and the two-phase system 'nonpolar organic solvent–aqueous solution', the stability order of the metal complexes is as follows:

$$[ML]^{3+} < [ML(H_2O)_6]^{3+} < [ML(NO_3)(H_2O)_4]^{2+} < < [ML(NO_3)_2(H_2O)_2]^{+} < [ML(NO_3)_3]$$

Table 3. Energies of extraction equilibria [Eqn (23)].[53]

Metal [M in Eqn (23)]	ΔG_{extr} /kcal mol^{-1}	
	L = **6d**	L = **6e**
Am	−42.4	−48.4
Eu	−42.2	−46.1

Narbutt *et al.*[55] reported a thorough theoretical DFT study on extraction of the Am^{3+} and Eu^{3+} ions from aqueous nitric acid solutions into 1,1,2-trichloroethane with the B3LYP hybrid functional, the PBE GGA-functional and the extended polarized split-valence TZ basis set 6-311G**. In order to reduce the computational cost of calculations, *N*,*N*,*N*′,*N*′-tetraethyl diglycolamide (TEDGA, 6b) was used as simplified model for TODGA (**6d**). The relativistic effects were taken into account using the core potentials; also, the 5f-, 6d-, 7s- and 7p-AOs for Am and the 4f-, 5d-, 6s- and 6p-AOs for Eu were treated explicitly with the complementary pseudorelativistic basis set for Eu and a valence basis set for Am. Relativistic effects were included in the ZORA approximation while the solvent effects were considered using the COSMO approach. The ionization potentials were calculated both ignoring and including the spin–orbit coupling. The nature of chemical bonding was analyzed using the Mulliken atomic charges in the NBO approximation and following Bader's approach 'Atoms in Molecule' (QTAIM).[63] Calculations of the 1 : 3 cationic complexes $[M(\mathbf{6d})_3]^{3+}$ reproduced the tridentate nature of all ligands in the inner coordination sphere of the metal. The metals are characterized by C.N. 9 and their coordination polyhedra represent twisted tricapped trigonal prisms. The bonds of the metals with the carbonyl oxygen atoms (R_{Eu-O} = 2.42 Å and R_{Am-O} = 2.46 Å) are much shorter than the bonds with the ether oxygen atoms (R^{l}_{Eu-O} = 2.62 Å and R^{l}_{Am-O} = 2.6 Å). The types of ligand coordination and the optimized structure of the cation $[Am(\mathbf{6b})_3]^{3+}$ are shown in Fig. 8.

The structure of the complexes $[M(6b)_3]^{3+}$ was not studied by X-ray diffraction, but the metal–oxygen interatomic distances in the europium complex and the type of the coordination polyhedron are, taking account of the ionic radii difference between two ions, in good agreement with those determined experimentally[64] for the cationic lanthanum complex with *N*,*N*,*N*′,*N*′-tetra(isolutyl)diglycolamide (TiBDGA), $[La(TiBDGA)_3]^{3+}$. An analysis of the electron density redistribution between the ligands and the central atom using Mulliken atomic charges revealed a pronounced ligand-to-metal electron transfer with greater involvement of the amide (carbonyl) oxygen atoms (O_{am}) rather than the ether oxygen atom (O_{eth}). This is a clear indication of noticeable covalency of the metal–oxygen coordination bonds. The Wiberg indices are indicative of even more pronounced covalency, being lower for the $M-O_{eth}$ bonds (0.13 for M = Am and 0.10 for M = Eu) than for the $M-O_{am}$ bonds (0.23 for M = Am and 0.19 for M = Eu). Interesting results were obtained in the orbital analysis (Table 4). As can be seen, the populations of the 7s/6s- and 5f/4f-AO of both metals differ only slightly from the canonical values, 0 and 6, respectively. The electron density is mainly transferred to the 6d/5d-AOs that make the major contribution to the covalency, which is much higher for americium.

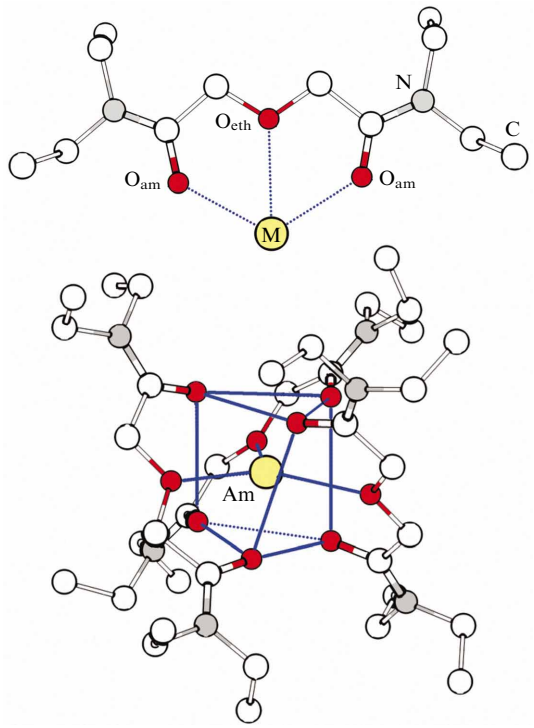


Figure 8. Type of ligand coordination and the optimized structure of $[Am(\mathbf{6b})_3]^{3+}$ cation.[55]

Table 4. Charge distribution on metal AOs in complexes $[M(\mathbf{6b})_3]^{3+}$.[55]

Complex	Partial charges
$[Am(\mathbf{6b})_3]^{3+}$	[core] 7s(0.14) 5f(6.13) 6d(0.71) 7p(0.01)
$[Eu(\mathbf{6b})_3]^{3+}$	[core] 6s(0.13) 4f(6.07) 5d(0.61) 6p(0.01) 6d(0.05)

Based on the results of analysis, the authors[55] drew a general conclusion of crucial importance, namely, the question as to what are the AOs responsible for the covalent contribution to the coordination bonds of the f-metals (actinides and lanthanides) requires detailed consideration using various methods of analysis in each particular case. An *a priori* statement that the major contribution comes from the f-AOs cannot stand up under criticism. The situation is governed by the energies and nodal properties of the metal and ligand orbitals participating in chemical bonding. Correct energy estimates showed that the complex cations $[Eu(\mathbf{6b})_3]^{3+}$ are more thermodynamically stable than $[Am(\mathbf{6b})_3]^{3+}$ in the gas phase, but the inclusion of solvation effects and the difference between the transfer energies of these ions from the aqueous phase to trichloroethane give rise to some selectivity for americium ions, which agrees with experimental data.

Concluding our consideration of the results of theoretical modelling of tridentate donor ligands with oxygen centres and their complexes with actinides and lanthanides, mention may be made of two more interesting studies reported by researchers from India[56,58] and devoted to modelling of binding the Eu^{3+} and Am^{3+} ions to a single-walled carbon nanotube (SWCNT) functionalized with diglycolamide (DGA). A $HO_2CCH_2OCH_2C(O)NH$ fragment was attached to the nanotube wall through a linker $CH_2CH_2NHC(O)-CNT$. Such a functionalized nanotube was synthesized earlier and used for extraction of the UO_2^{2+} and Th^{4+} ions from aqueous solutions.[65,66] Diglycolic acid monamides as anionic tridentate ligands appeared to be efficient extractants for the separation of actinides and lanthanides with high affinity for the lanthanide ions.[67–69]

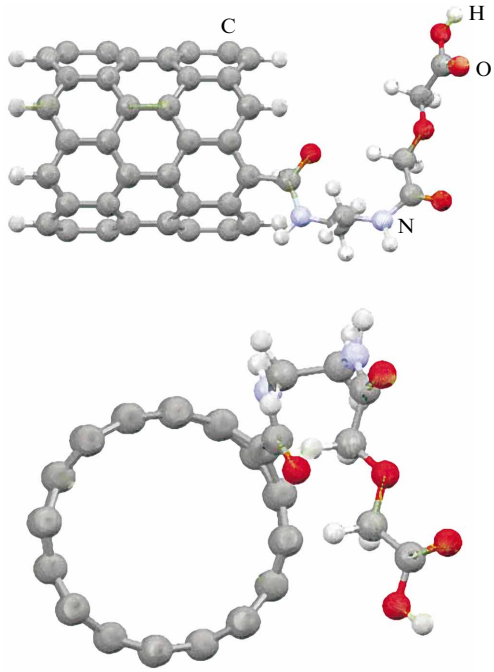


Figure 9. Optimized geometry of the model fragment of carbon nanotube {DGA(8.0)SWNT}.[58]

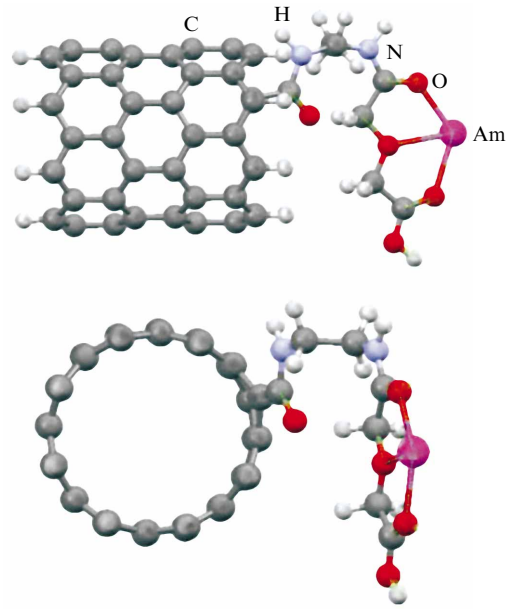


Figure 10. Optimized geometry of Am^{3+} complex with carbon nanotube {DGA(8.0)SWNT}.[58]

Density functional calculations were performed with the BP86 GGA-functional, a polarized split-valence basis set and the relativistic effective core potentials with 28 electrons in the core for Eu and 60 electrons in the core for Am. Energy calculations of the structures optimized with the BP86 functional were also carried out using the B3LYP hybrid functional and the TZVP basis set. The solvent effects were included using the COSMO approach. It is noteworthy that calculations were performed in the first step of the study with prognostic purposes prior to carrying out the experimental tests.

The optimized geometry of the model fragment of the nanotube {DGA(8.0)SWNT} (four unit cells with a tube length of 5.78 Å and a width of 6.40 Å) with the functional group is shown in two projections in Fig. 9, while the optimized structure of the complex with the Am^{3+} ion is presented in Fig. 10. The complex with the Eu^{3+} ion is structurally similar. As in the studies considered above,[53, 55] the bonds of the metal ions with the ether oxygen atoms in the complexes appeared to be longer (2.520 Å for Eu^{3+} and 2.596 Å for Am^{3+}) than the bonds with the carbonyl oxygen atoms (2.292 and 2.391 Å for Eu^{3+}; 2.324 and 2.419 Å for Am^{3+}). Also, the Eu–O bonds in these complexes are shorter than the Am–O bonds in accordance with the ionic radii difference. The binding energy (ΔE) of the Eu^{3+} ion obtained from gas-phase calculations is much higher than that of the Am^{3+} ion (-600.98 *vs.* -550.44 kcal mol^{-1}, respectively). The Gibbs energy differences (ΔG) are also large (-583.59 and -534.65 kcal mol^{-1}, respectively). The Eu^{3+} and Am^{3+} ions are bound in the aqueous phase. As should be expected, the inclusion of hydration effects abruptly decreases the thermal effect of binding and the ΔG values (-23.13 kcal mol^{-1} for the Eu^{3+} ion and -0.22 kcal mol^{-1} for the Am^{3+} ion). However, the calculations were carried out ignoring the fact that the Eu^{3+} and Am^{3+} ions are extracted from solutions which also contain nitrate anions as counterions. In this connection, the Gibbs energies were re-estimated taking account of the counterions using Eqn (24).

$$M^{3+}_{(aq)} + 3\,NO^{-}_{3\,(aq)} + \text{CNT-DGA}_{(aq)} \overset{\Delta G_{extr}}{\rightleftharpoons} \rightleftharpoons [\text{CNT-DGA}-M(NO_3)_3]_{(aq)} \quad (24)$$

The results obtained in this case were opposite to those mentioned above, namely, one has $\Delta G = -52.7$ kcal mol^{-1} for Eu^{3+} and 762.7 kcal mol^{-1} for Am^{3+}.

The experimentally determined [58] distribution ratios of the Eu^{3+} and Am^{3+} ions between the aqueous phase and the solid phase (nanotube) are equal to 496 and 337 ml g^{-1}, respectively, being in qualitative agreement with the results of modelling carried out without inclusion of the nitrate counterions. Clearly, ambiguity of the results is due to incompleteness of the chemical model. First of all, one should take into account the fact that the nanotube is a mono-anionic ligand, and the number of nitrate ions in the complex with the nanotube should be equal to two. Nevertheless, both studies carried out by researchers from India [56, 58] seems to be useful and valuable.

V. Complexes with aminopolycarboxylic acids

The most widely used aminopolycarboxylic acids (complexones) include ethylenediamine-*N*,*N*,*N*′,*N*′-tetraacetic acid (EDTA) and diethylenetriamine-*N*,*N*,*N*′,*N*″,*N*″-pentaacetic acid (DTPA) which are utilized in, *e.g.*, extraction processes. The latter compound is used as ligand for the separation of actinides and lanthanides in the TALSPEAK process and its recently proposed modification

called 'reversed TALSPEAK' process.[70, 71] In the latter case, the actinides and lanthanides are co-extracted from a 0.1 M HNO_3 solution into the organic phase using 1 M solution of bis(2-ethylhexyl) phosphoric acid (HDEHP). Then, americium and curium are selectively re-extracted from the organic phase to the aqueous solution containing DTPA (0.05 mol litre^{-1}) and lactic acid (1.5 mol litre^{-1}).$^{-1}$ The separation factors of An^{3+}/Ln^{3+} can be as high as 100 and more. The structure of the Am^{3+} and Nd^{3+} complexes with DTPA and the nature of the experimentally observed selectivity of complexation was theoretically studied by DFT methods.[72] The system $[M^{3+}(DTPA)H_2O]^{2-}$ (M = Nd, Am) was modelled using the B3LYP functional, the *aug*-cc-pVDZ basis set and relativistic pseudopotentials and analyzed using the NBO approach and according to Bader. The solvation effects were considered within the framework of the PCM model.

Calculations correctly reproduced the geometry of the complexes. The coordination spheres of the metals include six oxygen atoms from the carboxylate groups and three nitrogen atoms. The interatomic distances r(C–N) and r(C–O) are somewhat longer than the experimentally determined ones. The r(C–N) and r(C–O) values are almost equal for both cations having similar ionic radii (1.123 for Nd^{3+} and 1.115 Å for Am^{3+}). The complexation energy (ΔG) of Am^{3+} in the gas phase and in aqueous solution is higher than that of Nd^{3+} by 0.6 and 1 kcal mol^{-1}, respectively; this agrees with experimental data. A detailed analysis showed that the higher affinity of DTPA for Am^{3+} originates from higher covalency of the Am^{3+}–O and Am^{3+}–N bonds in the coordination site compared to that of the Nd^{3+}–O and Nd^{3+}–N bonds. It is noteworthy that the highest covalency was found for the Am^{3+}–O bonds. The f-AOs of both cations contribute slightly to corresponding MOs, the contribution being larger for the more diffuse 5f-AO of Am^{3+}. The major contribution comes from transfer of the electron density from the oxygen 2p-AO to the vacant d- and p-AOs of the metal ions; this is more pronounced for Am^{3+}. The results obtained in that excellent study emphasize again that conclusions on the nature of coordination bonds in the actinide and lanthanide complexes should be drawn only based on the results of comprehensive analysis in each particular case.

VI. Complexes of polydentate ligands based on N-heterocycles

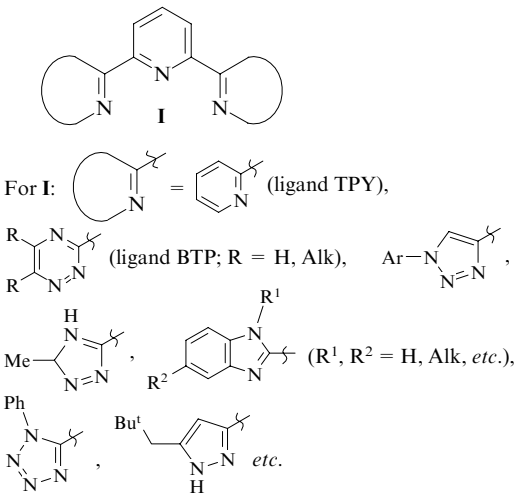
In the last decade, polydentate ligands based on aromatic heterocycles containing pyridine nitrogen atoms acting as donor centres have become a major type of extractants for the separation of lanthanides and MA. They offer a number of significant advantages. Most of them exhibit high oxidation, hydrolytic and radiation stabilities and form no solid products upon incineration in contrast to the extractants containing sulfur and phosphorus atoms. Based on rigid polycyclic structures, one can design ligands with tunable size of the coordination cavity. It is also important that synthetic methods in chemistry of N-heterocycles are well developed and allow one to synthesize structures of any degree of complexity from available reactants.

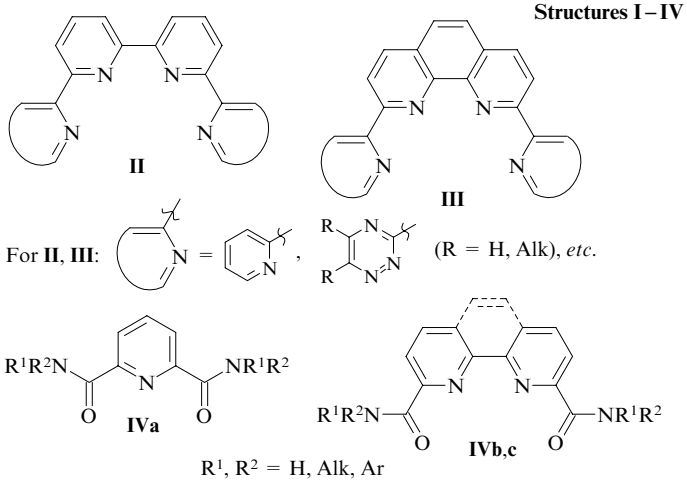
To date, a considerable body of experimental data on application of tridentate ligands based on 2,6-disubstituted pyridines (compounds of the general formula **I**) as well as tetradentate ligands based on 6,6′-disubstituted 2,2′-bipyridines (**II**) and 2,9-disubstituted 1,10-phenanthrolines (**III**) in the experiments on the extraction separation of lanthanides and MA has been accumulated. A particular group includes ligands containing, in terms of the HSAB concept, soft donor N-centres and harder O-centres, namely, pyridinedicarboxylic acid diamides (**IVa**), 2,2′-bipyridine-6,6′-dicarboxylic acid diamides (**IVb**) and 1,10-phenanthroline-2,9-dicarboxylic acid diamides (**IVc**). A number of modern studies on theoretical modelling of these ligands and their complexes with lanthanides and actinides are available.[73–88] Since some of them have been reviewed recently,[33] we will only briefly outline the materials reported in Ref. 33.

VI.1. Complexes of ligands based on 2,6-disubstituted pyridines

Both actinides and lanthanides form 1 : 3 complexes ($[ML_3]^{3+}$) with tridentate ligands in solutions in the presence of weakly coordinating solvents and counterions (perchlorate, *etc.*). In the presence of ions capable of forming strong coordination bonds (nitrate and chloride anions) and strongly solvating solvents (water), they can also form 1 : 1 and 1 : 2 complexes. The inner coordination sphere of the metals in these species comprises water molecules and counterions. In this case, one deals with a complex system of equilibria and theoretical assessment of selectivity in the

Structures I–IV



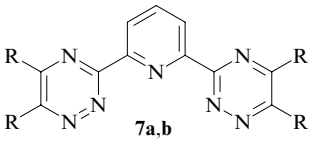


extraction separation should be done taking into account the fact that it depends on the physicochemical properties of all the complexes present in the solution and on the ratios of their concentrations.

Unrestricted Hartree–Fock calculations and DFT calculations with different functionals correctly reproduce the type of coordination polyhedra provided that the relativistic effects are included properly. The M–O and M–N coordination bond lengths are systematically overestimated to 0.1 Å as compared to the values obtained in the X-ray crystallography studies. This can be due to the crystal packing effects, to neglect of the influence of outer-sphere solvation of the complex in solution and to incomplete consideration of the electron correlation effects. As mentioned above, complex-forming ligands for the separation of actinides and lanthanides should rather strongly bind target ions, being of sufficiently low basicity. Among 2,6-disubstituted pyridines, this criterion is best met by bis(triazinyl)pyridines (BTP). These ligands and their complexes with americium and europium were studied in detail by quantum chemistry methods.

A thorough DFT study (PBE functional, TZ basis set, ZORA) of complexes of the type $[ML_3]$ [M = U^{3+}, Ce^{3+}; L = 2,2′:6′,2″-terpyridine (TPY); 2,6-bis(1,2,4-triazin-3-yl)pyridine (**7a**); 2,6-bis(5,6-dimethyl-1,2,4-triazin-3-yl)pyridine (**7b**)] was reported.[77]

Structures 7



7a,**b**

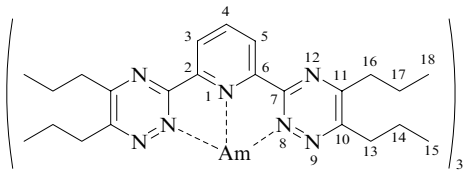
R = H (**a**), Me (**b**)

The calculated geometric parameters of the complexes are in very good agreement with experimental data determined by X-ray diffraction. Also, it was found that ligand **7b** forms stronger complexes with U^{3+} and Ce^{3+} than TPY and exhibits a higher affinity for U^{3+} and much higher selectivity ($SF_{An/Ln}$ is ~10 for TPY and ~150 for **7b**).[87] The donor methyl groups, which increase the electron density in the ligand and its basicity, also increase the metal binding energy and selectivity. Chemical bonds are mainly ionic, but the complex with uranium is characterized by higher covalency of the bonds; according to calculations, this is due to p-backdonation, *i.e.*, partial transfer of the electron density from the filled metal AOs to the ligand π*-MOs. This effect was not found in the cerium complexes.

Wipff and co-workers[78] carried out a DFT study of the effect of the substituents R in position 4 of pyridine ring on the basicity and extraction properties of substituted bis(triazinyl)pyridines 4-R-BTP used as ligands in the complexes $[Ln(4\text{-R-BTP})_3]$. The B3LYP functional, the 6-31G(d,p) basis set and pseudorelativistic core potentials were used. The effects of solvent were included within the framework of the PCM model. It was shown that the metal–ligand binding energy decreases as the ligand basicity decreases in the following order of 4-R-substituents: $NMe_2 > NH_2 > OMe > Ph > Bu^t > Me > H > F > Cl$.
For lanthanides, the metal–ligand binding energy changes as follows: $La^{3+} < Eu^{3+} < Yb^{3+}$. The relative contributions of the central pyridinyl and lateral triazinyl nitrogen atoms of the ligand to chemical bonding depend on the stoichiometry of the complex and on the ionic radius of the metal.

A direct proof of higher covalency of coordination bonds in the bis(triazinyl)pyridine complexes of Am^{3+} compared to isostructural lanthanide complexes was obtained by ^{15}N NMR spectroscopy. Adam *et al.*[88] synthesized a cationic complex $[Am(Pr^n\text{-BTP})_3]^{3+}$ (**8**) and labelled it with the isotope ^{15}N having a spin of 1/2.

Structure 8



8

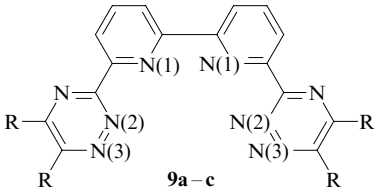
Two nitrogen atoms, N(1) and N(8), involved in the coordination of the americium ion, show very large upfield shifts (295 and 327 ppm, respectively) relative to positions of their signals in the ^{15}N NMR spectrum of a diamagnetic complex with lutetium. At the same time, the chemical shifts of the N(12) and N(9) atoms not involved in coordination are almost identical in the ^{15}N NMR spectra of the two complexes. A clear-cut temperature dependence of the chemical shifts of the N(1) and N(8) atoms was also observed. Both these facts indicate that abnormal chemical shifts of the coordinated nitrogen atoms are due to the direct Fermi contact interaction. This is only possible if the Am–N(1) and Am–N(8) bonds have a large s-contribution, thus being noticeably covalent.

VI.2. Complexes of ligands based on 6,6′-disubstituted-2,2′-bipyridines and 2,9-disubstituted 1,10-phenanthrolines

Compounds derived from 2,2′-bipyridine and 1,10-phenanthroline have long been used as ligands in coordination chemistry of main-group elements and transition metals. They are also utilized for the separation of MA and lanthanides. Numerous derivatives containing pyridine and triazine rings as substituents in positions 6, 6′ and 2, 9, respectively, have been synthesized to date. They exhibit very high separation factors ($68 < SF_{Am/Eu} < 400$) in the extraction in two-phase systems. There are a number of studies on theoretical modelling of these ligands and their complexes with lanthanides and actinides;[79,83,89–93] often, the extraction properties of the ligands in question are compared with those of 2,6-disubstituted pyridines.

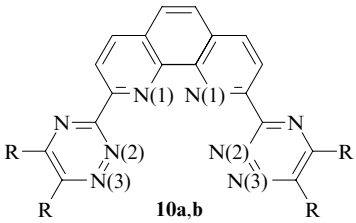
Tetradentate ligands 9 (R-BTBP) and 10 (R-BTPhen) form 1 : 1 and 2 : 1 complexes with lanthanides and actinides in solutions, the concentration ratio being dependent on the relative concentrations of the ligand and the metal ion, on solution pH and on the types and concentrations of the counterions. The structures of neutral complexes of the type $[ML(NO_3)_3]$ [M = Am^{3+}, Eu^3; L = 6,6′-bis(5,6-diethyl-1,2,4-triazin-3-yl)-2,2′-bipyridine, **9a**] were studied[79,89,90] by DFT using the B3LYP hybrid functional, the 6-31G(d) and 6-311G(d,p) basis sets and the effective core potentials, as well as by the MP2/6-311G(d,p) method for particular structures. In addition, Narbutt and Oziminski[79] calculated cationic complexes $[ML_2]^{3+}$. In all cases, metal atoms form coordination bonds with two N(1) atoms of the bipyridine or phenanthroline moiety and two lateral atoms, N(2). The

Structures 9, 10



9a–c

R = Et (**a**), H (**b**); R–R = $CMe_2(CH_2)_2CMe_2$ (**c**)



10a,b

R = H (**a**); R–R = $CMe_2(CH_2)_2CMe_2$ (**b**)

structure of the complex of 6,6′-bis(1,2,4-triazin-3-yl)-2,2′-bipyridine (**9b**) with americium nitrate is shown in Fig. 11. According to X-ray diffraction data and results of calculations, the M–N(2) bonds with the lateral nitrogen atoms in the complexes are shorter than the M–N(1) bonds, thus indicating a higher strength of the former. This conclusion is confirmed by analysis of the orbital populations and the electron density distribution in this type of complexes. In these species, nitrate anions act as bidentate ligands and the coordination number of the actinide and lanthanide atoms is 8.

The results of analysis of the electron density distribution and those of energy calculations show that the metal–ligand bonds in the complexes are mainly of ionic character. The metal–ligand bonds are more covalent in the americium complexes. In the extraction experiments, these ligands exhibit a high affinity for actinides [according to different sources, $SF_{Am/Eu}$ (**9b**) = 160 ± 16 and 200 ± 25]. However, gas-phase calculations predict that complex [Am(**9b**)$(NO_3)_3$] is less stable than [Eu(**9b**)$(NO_3)_3$]. As mentioned above, similar results that contradict experimental data on the extraction selectivity were also obtained for the complexes of Am^{3+} and Eu^{3+} with the P-donor (Cyanex-301) and O-donor [TODGA (**6d**), DMDHOPDA (**6e**)] ligands.[42, 53] It is an experimental fact[94] confirmed by high-level calculations[47, 48] that the hydration energy of the Eu^{3+} ion is much higher than that of the Am^{3+} ion (804.8 *vs.* 786.6 kcal mol^{-1}, respectively). The gas-phase metal–ligand binding energies (ΔE and ΔG) are respectively calculated as the E and G differences between the free ligands and the metal ions. In this case, the energies of hydration are ignored. Therefore, a model similar to those proposed in Refs 42 and 53 was used for correct description of the extraction from aqueous solutions.[79] According to the model, the ligand reacts with the nonahydrates $[M(H_2O)_9]^{3+}$ in the aqueous phase to give complexes of the types $[ML(NO_3)_3]$ and $[ML_2]^{3+}$ and then the complexes are transferred to the organic phase [Eqns (25) and (26)]. The separation factor $SF_{Am/Eu}$ was estimated from the Gibbs energy difference using expression (27). The model includes the hydration energies of the Eu^{3+} and Am^{3+} ions naturally and the estimated energies agree with experimental data.

$$[M(H_2O)_n]^{3+}_{(aq)} + L_{(org)} + 3\,NO^-_{3\,(aq)} \overset{K_{extr,\,1}}{\rightleftharpoons} [ML(NO_3)_3]_{(org)} + n\,H_2O_{(aq)} \quad (25)$$

$$[M(H_2O)_n]^{3+}_{(aq)} + 2\,L_{(org)} + 3\,NO^-_{3\,(aq)} \overset{K_{extr,\,2}}{\rightleftharpoons} [ML_2(NO_3)_y]^{(3-y)+}_{(org)} + (3-y)\,NO^-_{3\,(org)} + n\,H_2O_{(aq)} \quad (26)$$

$$-RT\ln SF_{Am/Eu} = \Delta G_{extr}(Am) - \Delta G_{extr}(Eu) = \Delta(\Delta G_{extr})_{Am/Eu} \quad (27)$$

Wipff and co-workers[89] modelled the behaviour of the bipyridine ligands and their protonated forms in the system 'acidic aqueous solution–organic solvent' by the molecular mechanics method. It was shown that free neutral ligands are not concentrated at the interface where complexation occurs, the interface being mainly covered with the protonated ligands. Therefore, complexation shold be treated as replacement of a proton in the cavity of the protonated ligand by the metal cation. This model provides an explanation for the slow extraction kinetics and for an increase in the distribution ratios with increasing acidity of the medium in certain systems.

The geometry of a ligand in the free state and in the complex with a metal can be significantly different. Therefore, the kinetics of complexation should depend strongly on the ligand 'pre-organization' energy which can be estimated as the Gibbs energy difference between the free ligand and the ligand in the complex. It is this feature that is responsible for higher efficiency of the phenanthroline ligands compared to the bipyridine ones in the extraction. The phenanthroline molecule adopts a rigid *cis*,*cis*,*cis*-conformation suitable for binding the cation. Full conformation maps of 6,6′-bis(1,2,4-triazin-3-yl)-2,2′-bipyridine and 2,9-bis(1,2,4-triazin-3-yl)-1,10-phenanthroline are available.[92] High 'pre-organization' energy of the bipyridine ligand (12 kcal mol^{-1}) in the chelation of the metal ion is mainly due to the changes in the molecular conformation as a result of rotation about the C(2)–C(2′) central bond. The influence of the 'pre-organization' energy of the ligands on the thermodynamics of complexation was considered in more detail using simpler model systems in another study.[81]

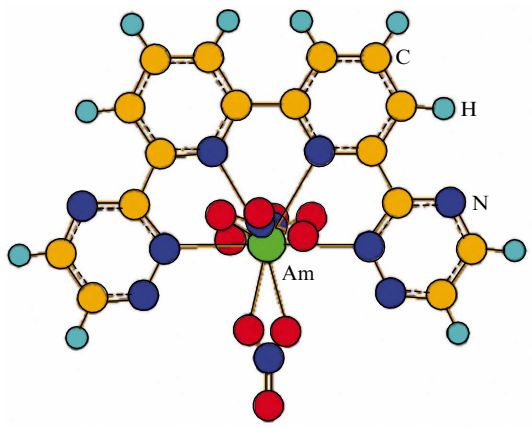


Figure 11. Structure of complex of 6,6′-bis(1,2,4-triazin-3-yl)-2,2′-bipyridine (**9b**) with americium nitrate [Am(**9b**)$(NO_3)_3$].[90]

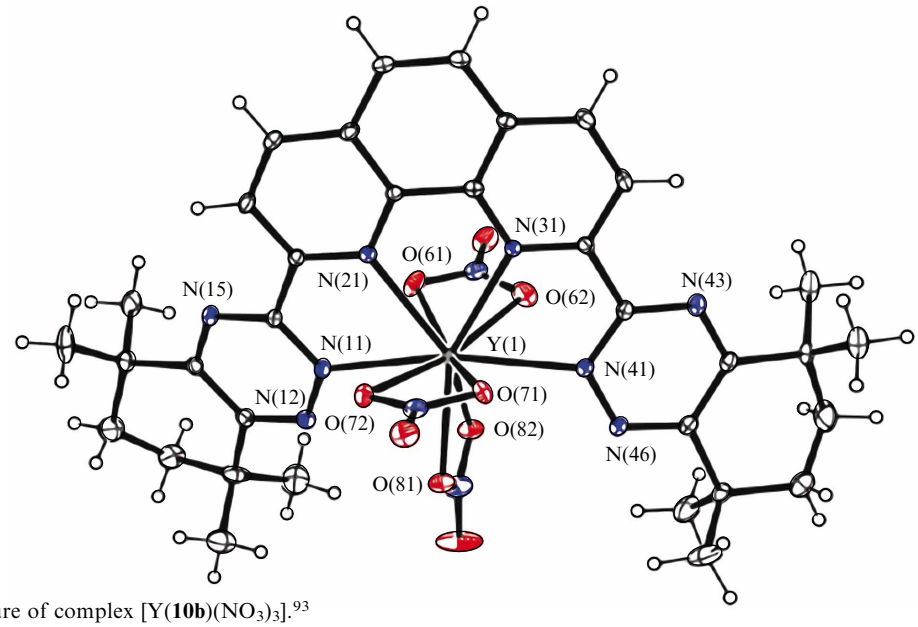


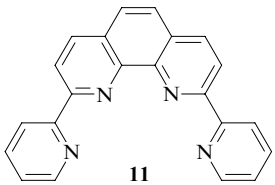
Figure 12. Structure of complex [Y(**10b**)$(NO_3)_3$].[93]

Researchers from China[90–92] as well as Lewis and coworkers[93] carried out detailed DFT studies of complexes of the types $[ML(H_2O)_4]^{3+}$ and $[ML(NO_3)_3]$ (M = Am, Eu; L = **9a**–**c**, **10a**,**b**, *etc.*) using the B3LYP functional, the 6-311G(d,p) basis set and relativistic core potentials. They calculated the free energies of formation and analyzed the electron density distribution, the MO energies and the nodal properties of the MOs. The structure of the complex [Y(**10b**)$(NO_3)_3$] determined by X-ray diffraction[93] is shown in Fig. 12.

According to these calculations, the gas-phase free energies of formation of the Eu^{3+} complexes with phenanthroline ligands ($[ML(NO_3)_3]$) are higher than those of the Am^{3+} complexes. However, like in other cases, the selectivity in the extraction experiments is governed by the higher relative stability of the americium complexes in solution, which is due to higher desolvation energy of $[Eu(H_2O)_9]^{3+}$ (see also Ref. 79). Within the framework of the model described by Eqns (25) and (26), calculations correctly reproduce the experimentally observed trends including the influence of substituents and ligand 'pre-organization' energies on the stability of the complexes.

Concluding our consideration of the extraction properties of the polyazine tetradentate ligands containing the 2,2′-bipyridine and 1,10-phenanthroline moieties, mention should also be made of a study[95] on the synthesis, experimental and theoretical investigations of complexes of 2,9-bis(pyrid-2-yl)-1,10-phenanthroline (**11**) with various lanthanide cations (La^{3+}, Pr^{3+}, Sm^{3+}, Gd^{3+}, Dy^{3+}, Er^{3+}, Yb^{3+}, Lu^{3+}), UO_2^{2+} cation and a number of alkaline earth metal cations. The authors of that study systematically examined how the size of the coordination cavity of the ligand and the ligand 'pre-organization' energy influence the stability constants of the metal complexes. In particular, taking calcium complexes as examples, it was shown that going from the conformationally flexible, 'non-pre-organized' 6,6′-bis(pyrid-2-yl)-2,2′-bipyridine to the conformationally rigid 2,9-bis(pyrid-2-yl)-1,10-phenanthroline (**11**) causes the stability constant of the complex in aqueous solution to increase by more than a decimal order of magnitude.

Structure 11



11

VI.3. Complexes of pyridine-2,6-dicarboxylic acid diamides, 2,2′-bipyridine-6,6′-dicarboxylic acid diamides and 1,10-phenanthroline-2,9-dicarboxylic acid diamides

A disadvantage of the polyazine ligands based on 2,6-disubstituted pyridines, 6,6′-disubstituted 2,2′-bipyridines and 2,9-disubstituted 1,10-phenanthrolines containing only soft donor N-centres and used in the extraction experiments consists in strong dependence of the distribution ratios (*D*) on the pH of the medium. Namely, the distribution ratios appreciably decrease as the concentration of nitric acid in the aqueous solution increases to more than 3 mol litre^{-1}. Pyridine-2,6-dicarboxylic (dipicolinic) acid diamides (**12**), 2,2′-bipyridine-6,6′-dicarboxylic acid diamides (**13**) and 1,10-phenanthroline-2,9-dicarboxylic acid diamides (**14**) are free from this drawback. These ligands also exhibit higher affinity for actinides. In particular, experiments[96] showed that ligands **12** containing one alkyl and one aryl substituent at the amide nitrogen atoms can be used for efficient extraction of actinides and lanthanides in the form of complexes $[ML(NO_3)_3]$ (M = Ln, An; L = 12) from solutions containing less than 6 mol litre^{-1} of nitric acid into polar organic solvents. Noteworthy is that the extraction coefficients increase rather than decrease with increasing acidity of the medium. Namely, on going from 1 M to 6 M HNO_3 they increase from 0.1 to 10 for extraction of Am^{3+} and from 0.01 to 1.5 for extraction of Eu^{3+}. The extraction properties of these ligands have been reviewed recently.[97]

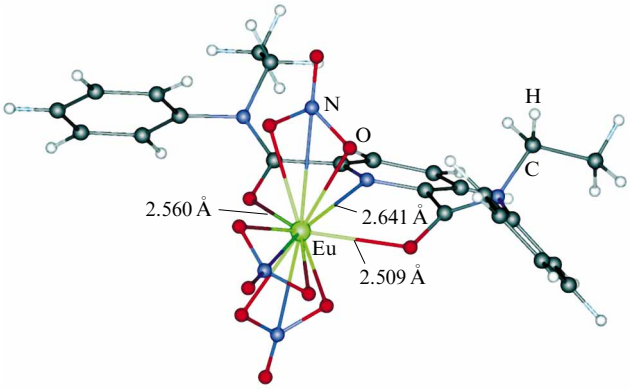


Figure 13. Optimized structure of complex [Eu(**12c**)$(NO_3)_3$].[98]

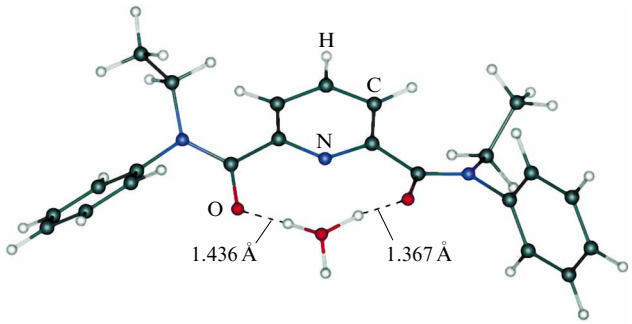


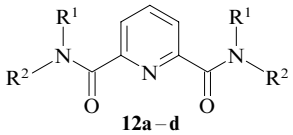
Figure 14. Optimized structure of protonated *N*,*N*′-diphenyl-*N*,*N*′-diethylpyridine-2,6-dicarboxamide [(**12c**)$(H_3O)]^+$ (Ref. 98).

The structures and properties of a large series of pyridine-2,6-dicarboxylic acid diamides (L) bearing different substituents at the amide nitrogen atoms and in the pyridine ring, including compounds **12a–d**, their complexes of the types $[ML]^{3+}$ and $[ML(NO_3)_3]$ (M = Eu, Am) and hydrates $[M(NO_3)_3(H_2O)_n]$ (n = 3, 4) were modelled by quantum chemistry methods within the framework of the DFT approach using the PBE functional and an extended relativistic full-electron basis set.[98] Gas-phase calculations excellently reproduce the geometry of the ligands (in the free state, the ligands adopt asymmetric unfolded conformations) and complexes $[ML(NO_3)_3]$ (M = Eu, Am) where the ligands adopt the *syn*,*syn*-conformations for convenient chelation of the metals. The Eu and Am ions are coordinated through two carbonyl oxygen atoms and the pyridine nitrogen atom. As an example, Fig. 13 presents the structure of the complex [Eu(**12c**)$(NO_3)_3$]. *A propos*, calculations reproduce an experimentally observed[99,100] feature of the geometry of this type of complexes, *viz*., deviation of the metal ion from the pyridine ring plane, and provide a relevant explanation for this subtle detail. Deviation of the carbonyl oxygen atoms from the pyridine ring plane owing to rotation about the C(2)–C(O) and C(6)–C(O) bonds violates conjugation between the carbonyl groups and the pyridine ring. An analysis showed that this causes the negative charges of the oxygen atoms and the energies of the M^{3+}–O bonds to increase because the bonding is mainly of electrostatic ionic character.

Since the formation of the europium and americium complexes with ligands occurs at the interface and involves protonated ligands, the structures of the $[L(H_3O)]^+$ species were calculated.[98] It is noteworthy that, according to calculations, the complexes also have nonplanar geometry. The hydroxonium ion forms two strong hydrogen bonds with the carbonyl oxygen atoms, while the nitrogen atom is not involved in the bonding. Figure 14 presents the structure of protonated *N*,*N*′-diphenyl-*N*,*N*′-diethylpyridine-2,6-dicarboxamide (**12c**).

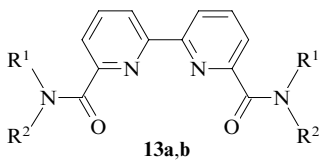
Modelling of the behaviour of free ligands and their protonated forms in the two-phase system water–octane by the molecular mechanics method showed[98] that the protonated ligand molecules $[L(H_3O)]^+$ are localized at the interface and their conformations are convenient for the replacement of hydroxonium ion by the metal cation to occur. At the same time, unprotonated ligand molecules reside in the organic phase and their concentration at the interface is very low. This made it possible to formulate a more complete model for extraction processes, which provides a consistent explanation for both the experimentally observed increase in the extraction coefficients with increasing acidity of the medium and the influence of the bulky hydrophobic anions, such as chlorinated cobalt dicarbollide (CCD), which cause the distribution ratios to increase and accelerate the extraction kinetics. As was assumed by Wipff and co-workers[89] for the complexes of lanthanides with R-BTBP and R-BTBPhen, the process begins with reversible protonation of the ligand which is localized at the interface [Eqn (28)]. Most probably, the counterion (in this case, the nitrate anion) residing in the aqueous phase forms a contact ion pair with the ligand. The exchange step involves replacement of hydroxonium ion in the protonated ligand by the metal ion and simultaneous displacement of water molecules from the inner coordination sphere of the metal ion [Eqn (29)]. Within the framework of this model, the influence of bulky hydrophobic anions becomes understandable. Being near the interface in the organic phase, the anions form solvent-separated ion pairs with the ligand bound to the hydroxonium ion and thus provide nucleophilic assistance to the attack of the metal ion and facilitate displacement of the hydroxonium ion from the coordination cavity of the ligand.

Structures 12–14



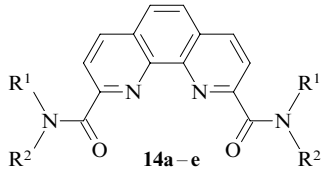
12a–d

$R^1 = R^2$ = Et (**a**); R^1 = Ph: R^2 = Me (**b**), Et (**c**); R^1 = Me, R^2 = 4-$MeOC_6H_4$ (**d**)



13a,b

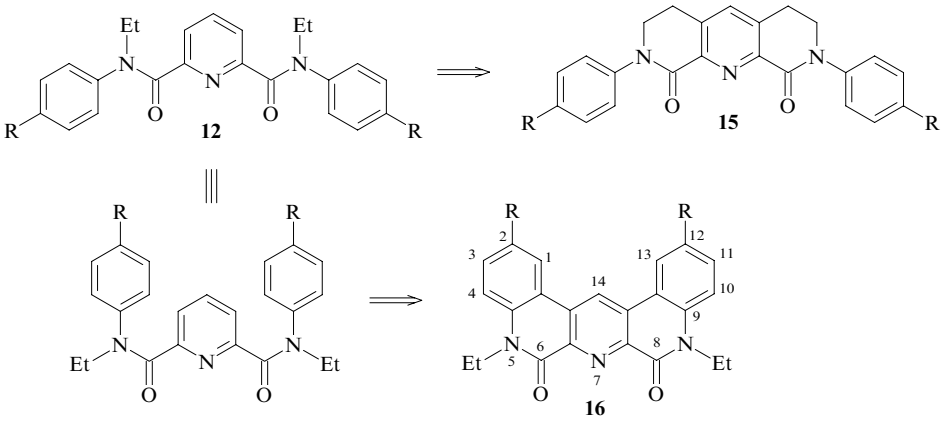
R^1 = Et, R^2 = Ph (**a**); $R^1 = R^2$ = Bu^n (**b**)



14a–e

R^1 = Et, R^2 = 4-MeC_6H_4 (**a**), $R^1 = R^2$ = Et (**b**), H (**c**), Bu^i (**d**); R^1 = H, R^2 = n-$C_{10}H_{21}$ (**e**)

Scheme 2



$$L + [H_3O]^+ \rightleftharpoons [LH_3O]^+ \quad (28)$$

$$[LH_3O]^+ + [M(NO_3)_3(H_2O)_n] \rightleftharpoons \rightleftharpoons [ML(NO_3)_3] + H_3O^+ + n\,H_2O \quad (29)$$

$n = 3, 4$

According to calculations,[98] the experimentally determined higher stability of the complexes containing one aryl and one alkyl substituent at the amide nitrogen atoms compared to the complexes of *N*,*N*,*N*′,*N*′-tetraalkylamides ('aryl strengthening effect') is due to the smaller energy difference between the *syn*,*syn*-conformations adopted by the ligands in the complexes and the unfolded conformations correspoding to minimum of the total energy of free ligands (ligand 'pre-organization' energy).

The thermodynamic parameters of the equilibria (28) and (29) were evaluated using the overall Eqn (30) for the gas phase and the separation factors were calculated conventionally using Eqn (31).

$$L + [M(NO_3)_3(H_2O)_n] \rightleftharpoons [ML(NO_3)_3] + n\,H_2O \quad (30)$$

$n = 3, 4$

$$-RT\ln SF_{Am/Eu} = \Delta\Delta G_{298}(Am - Eu) \quad (31)$$

Here, the effect of solvent is not included in explicit form. First of all, the approach ignores specific solvation, that is, the formation of hydrogen bonds by the ions and complexes in the aqueous phase, although these bonds undoubtedly play the key role. In spite of this, the calculated separation factor $SF_{Am/Eu} = 2.3$ appeared to be close, in the order of magnitude, to the experimental value $SF_{Am/Eu} \approx 6$. Good agreement seems to be due to the fact that the solvent influences the two isostructural complexes in almost the same fashion.

The ligand 'pre-organization' energies calculated for pyridine-2,6-dicarboxylic acid diamides **12** are rather high, *viz.*, 19–22 kcal mol^{-1} for the compounds containing four alkyl substituents at nitrogen atoms and 16.0–16.6 kcal mol^{-1} for the compounds containing one alkyl and one aryl substituent at each amide nitrogen atom. In this connection, it was assumed[98] that dilactams (their simplest representatives are ligands **15** characterized by almost zero 'pre-organization' energies) should exhibit much better extraction properties (Scheme 2).

Calculations predict that the extraction coefficients and the separation factor $SF_{Am/Eu}$ should increase by about two and one orders of magnitude, respectively, on going to this more conformationally rigid structure. The synthesis of dilactams **15** has not been reported as yet; however, methods for the synthesis of dilactams **16** of more complex structure containing a structurally similar fragment are available.[101] Calculations of the model lactam (**16a**, R = Me) and its complexes with Eu^{3+} and Am^{3+} were carried out using the same approach as that utilized for pyridine-2,6-dicarboxylic acid diamides.[98] Since the composition of the complexes was *a priori* unknown, calculations were performed for the 1 : 1 and 2 : 1 complexes of the types $[ML(NO_3)_3]$ and $[ML_2(NO_3)_3]$ [M = Eu, Am; L = **16a** (R = Me)] resulting from the equilibrium reactions (32) and (33).

$$[M(NO_3)_3(H_2O)_4] + L \rightleftharpoons [ML(NO_3)_3] + 4\,H_2O \quad (32)$$

$$[M(NO_3)_3(H_2O)_4] + 2\,L \rightleftharpoons [ML_2(NO_3)_3] + 4\,H_2O \quad (33)$$

The thermodynamic parameters were evaluated as in Ref. 98 and the separation factors were calculated conventionally using Eqn (31).

The Gibbs energies of formation of the complexes $[ML(NO_3)_3]$ and $[ML_2(NO_3)_3]$ [M = Eu, Am; L = **16a** (R = Me)] and the calculated separation factors $SF_{Am/Eu}$ are listed in Table 5.

The calculated Gibbs energies of formation (ΔG^{eq}_{298}) of the complexes $[ML(NO_3)_3]$ appeared to be ~30 kcal mol^{-1} higher than those of the complexes of the open-structure diamides **12**. This suggests that the distribution ratios for extraction of the complexes should increase by at least two orders of magnitude. Dilactams **16a–c** [R = Me (**a**), Et (**b**), n-C_6H_{13} (**c**)] have been synthesized recently.[102, 103] Extraction of Eu^{3+} and Am^{3+} from aqueous nitric acid solutions to *m*-nitrobenzotrifluoride (*m*-trifluoromethylnitrobenzene, F-3), chloroform and dichloroethane at different nitric acid

Table 5. Gibbs energies of formation of complexes $[M(\mathbf{16a})(NO_3)_3]$ and $[M(\mathbf{16a})_2(NO_3)_3]$ and separation factors (M = Eu, Am; R = Me) (author's data; unpublished).

Complex	ΔG^{eq}_{298} /kcal mol^{-1}	$SF_{Am/Eu}$
$[Eu(\mathbf{16a})(NO_3)_3]$	−34.7	40.1
$[Am(\mathbf{16a})(NO_3)_3]$	−36.9	
$[Eu(\mathbf{16a})_2(NO_3)_3]$	−24.4	29.1
$[Am(\mathbf{16a})_2(NO_3)_3]$	−26.4	

Table 6. Distribution ratios and separation factors in extraction of Eu^{3+} and Am^{3+} using 0.01 M solutions of ligand **16c** (R = n-C_6H_{13}) in three different solvents at different concentrations of nitric acid.[102, 103]

$[HNO_3]$ /mol litre^{-1}	F-3			$CHCl_3$			$C_2H_4Cl_2$		
	D_{Am}	D_{Eu}	$SF_{Am/Eu}$	D_{Am}	D_{Eu}	$SF_{Am/Eu}$	D_{Am}	D_{Eu}	$SF_{Am/Eu}$
1	12	0.8	15	0.2	0.01	20	3	0.2	15
2	22	1.2	18	0.5	0.04	13	7	0.4	18
3	44	1.9	23	1.0	0.08	13	14	0.8	18
4	70	2.7	26	1.9	0.18	11	24	—	—
5	120	4.5	27	3.8	0.36	11	49	2	25
6	150	4.9	31	8.5	0.79	11	22	—	—

concentrations was studied[102, 103] taking ligand **16c** (R = n-$C_{16}H_{13}$) (Table 6) as an example.

An analysis of the dependence of D_{Am} and D_{Eu} on the concentration of the ligand showed that both metals are extracted as complexes $[ML_2(NO_3)_3]$ (M = Eu, Am). Thus, the results of calculations are in excellent agreement with experimental data. Very high D_{Am} and D_{Eu} values deserve particular attention because they are about three orders of magnitude higher than the corresponding values obtained[104] for the best ligand 12 (R^1 = Et, R^2 = 4-$F_3CC_6H_4$).

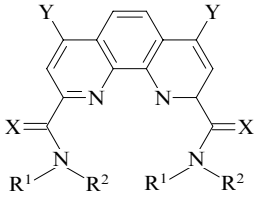
Studies[105–109] on the experimental and theoretical research into the extraction properties of 1,10-phenanthroline-2,9-dicarboxylic acid diamides were published nearly simultaneously. Researchers from China[105] reported very high selectivity of 1,10-phenanthroline-2,9-dicarboxylic acid *N*,*N*′-diethyl-*N*,*N*′-di(*p*-tolyl)diamide (**14a**) for MA in the extraction from strongly acidic solutions. The separation factors for extraction from 1 M nitric acid were as follows: $SF_{Am/Eu}$ = 67, $SF_{Th^{IV}/Eu}$ = 2277 and $SF_{U^{VI}/Eu}$ = 227. The structures of the complexes of ligand **14a** and corresponding tetraethyl derivative **14b** with Eu^{3+}, Am^{3+}, $[UO_2]^{2+}$, $[NpO_2]^+$ and $[PuO_2]^{2+}$ cations were thoroughly studied[105,106] by DFT methods using the B3LYP hybrid functional, the 6-311G(d,p) basis set and pseudorelativistic core potentials. Geometry optimization of the complexes $[AnO_2L(NO_3)]^{n+}$ (An = U^{6+}, Np^{5+}, Pu^{6+}; n = 0, 1) and $[PuL_2(NO_3)_2]^{2+}$ and $[PuL(NO_3)_4]^{2+}$ was performed for the gas phase; only electrostatic solvent effects were considered using the COSMO approach with water and cyclohexanone being model solvents. Both ligands in the complexes act as tetradentate species and coordinate the metal ions through two nitrogen atoms of the phenanthroline moiety and two carbonyl oxygen atoms. Calculations reproduce the geometry of the complexes with high accuracy. The orbital population analysis and the NBO analysis showed that the metal–ligand bonds M ← N and M ← O are mainly of ionic character. Noticeable covalent contribution was found only for the actinide complexes. The An ← O bonds appeared to be more covalent.

Estimation of thermodynamic parameters showed that the metal–ligand binding energies in the actinide complexes change as follows: $Pu^{IV} > U^{VI} > Pu^{VI} > Np^{V}$. This is in agreement with experimental data. Although the character of bonding and the electron density distribution in the complexes of both ligands were almost identical, compound **14a** forms stronger complexes. Thus, the effect of 'anomalous aryl strengthening' also manifests itself in these systems.

Researchers from India theoretically studied[107] complexes of 1,10-phenanthroline-2,9-dicarboxylic acid diamide (**14c**), its *N*,*N*,*N*′,*N*′-tetraisobutyl (**14d**) and *N*,*N*′-didecyl (**14e**) analogues, as well as 1,10-phenanthroline-2,9-dithiocarboxylic acid diamide (**17**) with the Am^{3+} and Eu^{3+} cations of the types $[ML_2]^{3+}$, $[ML_2(NO_3)]^{2+}$ and $[ML_2(NO_3)_3]$. They carried out DFT calculations using the BP-86 GGA-functional, the B3LYP hybrid functional, the TZ2p basis set and the COSMO approach. Earlier,[108] they studied complexes of 1,10-phenanthroline-2,9-dicarboxylic acid within the framework of the same approximations. Only the total electronic energies were calculated and compared, the Gibbs energies were not calculated. Calculations predicted a lower stability for the Am^{3+} complexes of the $[ML_2]^{3+}$ type in the gas phase compared to the Eu^{3+} complexes, but the situation is reversed on going to complexes of the type $[ML_2(NO_3)]^{2+}$. Having synthesized ligands **14d**,**e**, the authors carried out experiments on extraction of Am^{3+} and Eu^{3+} from 0.01 M HNO_3 solutions into a mixture of 2-bromo-octanoic acid and dodecane and showed that both these ligands exhibit some selectivity for Am^{3+}, but the distribution ratios were very low.

Recently,[109] we have reported the results of DFT calculations (PBE functional, full-electron relativistic TZ2p basis set) of the structures of *N*,*N*′-diethyl-*N*,*N*′-diphenyl-4,7-dichloro-1,10-phenanthroline-2,9-dicarboxylic acid diamide (**18a**) and its complexes with lanthanides and americium of the type [M(**18a**)$(NO_3)_3$].

Structures 17, 18



17, **18a**,**b**

X = S, Y = R^1 = R^2 = H (**17**);
X = O, Y = Cl, R^1 = Et:
R^2 = Ph (**18a**), 4-n-$C_6H_{13}C_6H_4$ (**18b**)

Donor ligands capable of forming strong complexes with Ln^{3+} ions can be conditionally divided into three groups with respect to the behaviour of the stability constants of the complexes with increasing atomic number of the lanthanide:

— monotonic increase in stability constants throughout the series from La^{3+} to Lu^{3+} as a consequence of the increase in the charge density on the central metal ion with decreasing ionic radius; this is the largest group; examples are provided by all N-heterocyclic ligands based on 2,6-disubstituted pyridines (see above);

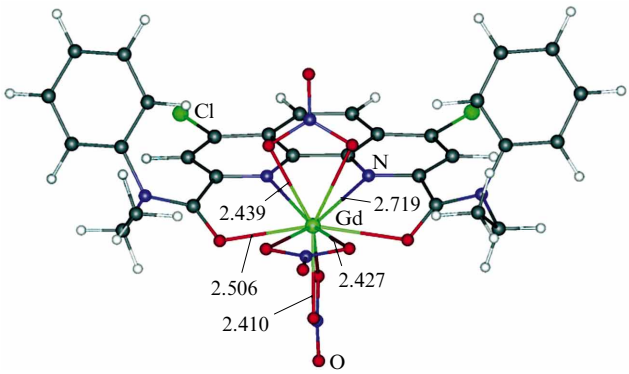


Figure 15. Optimized structure of complex [Gd(**18a**)$(NO_3)_3$].[109]

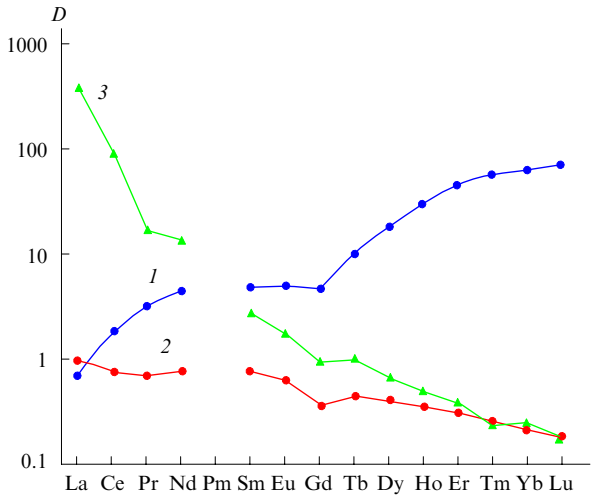


Figure 16. Distribution ratios for the extraction of lanthanide ions in the system 3 M HNO_3 – F-3.
Extractants: 0.2 M solution *N*,*N*′-diethyl-*N*,*N*′-di(*o*-tolyl)pyridine-2,6-dicarboxamide (*1*), 0.1 M solution of diamide **13a** (*2*) and 0.05 M solution of ligand **18b** (*3*).[109]
Different extractant concentrations were used to obtain close *D* values for easy comparison.

— an increase in the stability constants, reaching a plateau and subsequent decrease for heavier lanthanides; these ligands are more rarely to occur; an example is provided by 2,9-bis(pyrid-2-yl)-1,10-phenanthroline (**11**);[95] and

— a decrease in the stability constants throughout the series; a rare case; examples are provided by functionalized azacrown ethers.[110]

Alyapyshev *et al.*[111] studied extraction of lanthanides by 2,2′-bipyridine-6,6′-dicarboxylic acid diamides (**13a**,**b**) and showed that the distribution ratios (*D*) of ligands of this type somewhat decrease with increasing atomic number of the lanthanide, although the dependence is not well pronounced. Undoubtedly, the reason is that diamides **13** have large coordination cavities that are more appropriate for binding cerium subgroup cations with large ionic radius. Choosing compound **18a** as an object for theoretical study, we were guided by the assumption that 1,10-phenanthroline-2,9-dicarboxylic acid diamides having more rigid geometry should bind light lanthanides more selectively than diamides **13**.

According to calculations, all complexes with compound **18a** acting as tetradentate N,N,O,O-ligand are structurally similar. The calculated structure of the gadolinium complex is presented in Fig. 15. Like in the complexes of pyridine-2,6-dicarboxylic acid diamides (see text above and Fig. 13), the metal ions deviate from the plane of the donor ligand π-system. However, the angles of deviation of the Ln^{3+} ions from the plane of the rigid phenanthroline system are merely 6–8°. Owing to the rigid ligand geometry, the interatomic distances in the coordination site vary only slightly on going throughout the series from La^{3+} to Lu^{3+}. For instance, the Ln^{3+}–N(1) and Ln^{3+}–N(10) distances lie in a relatively narrow range 2.82–2.63 Å, while the shorter distances, Ln^{3+}–O(CO), lie in the range 2.62–2.47 Å. The metal–ligand binding energies (E^b, G^b) were calculated as the total electronic energy differences and the Gibbs energy differences between the complexes [M(**18a**)$(NO_3)_3$] and anhydrous nitrates [M$(NO_3)_3$] (Table 7).

The data of Table 7 clearly demonstrate a general trend, namely, a decrease in the binding energy with increasing atomic number of the lanthanide, the trend being most pronounced for the early lanthanides from Ce to Sm. Calculations were carried out for the gas phase ignoring potentially significant effects of the medium. Therefore, the results obtained are inappropriate for estimating the separation factors and should be considered only qualitatively. Nevertheless, they substantiated the assumption of high selectivity of ligand **18a** for the light lanthanides.

We synthesized[109] a series of 1,10-phenanthroline-2,9-dicarboxylic acid diamides and studied the extraction properties of ligand **18b** for lanthanides, americium and

Table 7. Ligand–metal[a] binding energies in complexes [M(**18a**)$(NO_3)_3$].[109]

M	E^b (G^b) /kcal mol^{-1}	ΔE_{Ce-M} (ΔG_{Ce-M}) /kcal mol^{-1}	M	E^b (G^b) /kcal mol^{-1}	ΔE_{Ce-M} (ΔG_{Ce-M}) /kcal mol^{-1}
Ce	63.2 (43.8)	0.0	Tb	55.4 (35.2)	7.8 (8.6)
Pr	56.9 (38.5)	6.3 (5.3)	Dy	54.0 (33.8)	9.2 (10.0)
Nd	55.3 (35.7)	7.9 (8.1)	Ho	53.1 (33.1)	10.1 (10.7)
Pm	55.2 (35.6)	8.0 (8.2)	Er	54.2 (34.0)	9.0 (9.8)
Sm	54.3 (35.4)	8.9 (8.4)	Tm	51.1 (31.3)	12.2 (12.5)
Eu	56.1 (36.6)	7.1 (7.2)	Yb	50.7 (31.2)	12.5 (12.6)
Gd	56.4 (36.2)	6.8 (7.6)	Lu	51.8 (29.7)	11.4 (14.1)

[a] ΔE and ΔG denote the differences with corresponding quantities for the cerium complex.

curium in two-phase systems 'aqueous nitric acid solutions–*m*-nitrobenzotrifluoride' at HNO_3 concentrations from 1 to 5 mol litre^{-1}. Ligand **18b** differs from its analogue **18a** only in that the phenyl moieties at the amide nitrogen atoms bear n-hexyl substituents introduced into distant *para*-positions to enhance the solubility in organic solvents. Figure 16 presents the distribution ratios for extraction of the lanthanide ions in the system 3 M HNO_3 – F-3 for three extractants belonging to diamides of N-heterocyclic dicarboxylic acids considered in this Section, *viz*., *N*,*N*′-diethyl-*N*,*N*′-di(*o*-tolyl)pyridine-2,6-dicarboxamide and compounds **13a** and **18b**. As can be seen, experimental data are in good agreement with the results of calculations. Dramatic differences in the extraction properties of the three ligands can be explained with ease using the results of theoretical study and experimental data. As was assumed, pyridine-2,6-dicarboxylic acid diamides with small coordination cavities preferentially bind heavier lanthanides having small ionic radii. 2,2′-Bipyridine-6,6′-dicarboxylic acid diamides have much larger coordination cavities, but conformational flexibility of these ligands due to rotation around the central bond, C(2)–C(2′), allows them to 'tune' to different cations. The rigid, more 'pre-organized' ligand **18b** is much more appropriate for binding lighter lanthanides with large ionic radii. Figure 17 presents the distribution ratios *D* for extraction of the lanthanide and americium ions in the same system at different HNO_3 concentrations.

The separation factors $SF_{Am/Eu}$ obtained for diamide **18b** are close to those reported for diamide **14a** synthesized by researchers from China.[105] The SF_{Ln^1/Ln^2} values for the separation in pairs of neughrouring lanthanides using extraction from 1 M HNO_3 by ligand **18b** are as follows: 2.17 for La/Ce, 3.5 for Ce/Pr, 2.8 for Pr/Nd, 3.9 for Nd/Sm, 2.3 for Sm/Eu and 3.0 for Eu/Gd. They are much higher than those obtained using other extractants in similar conditions, being close to record-high values. The extraction coefficients for compound **18b** are tenfold and more higher than corresponding values for TBP and *N*,*N*-diisobutylcarbamoylmethyl(octyl)phenylphosphine oxide in the whole range of the HNO_3 concentrations studied. The observed increase in *D* values with increasing acid concentration substantiates our model[98] for extraction mechanism, according to which extraction proceeds at the interface as replacement of hydroxonium ion in the coordination cavity of the ligand by the metal ion. Ligand **18b** also exhibits high selectivity in the extraction separation of americium and curium in the same system ($SF_{Am/Cm} = 7$).

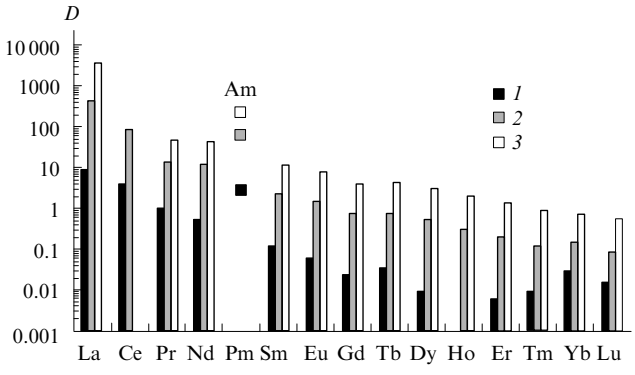


Figure 17. Distribution ratios of Ln^{3+} and Am^{3+} for extraction from aqueous solutions by solutions of ligand **18b** in F-3 at three different concentrations of HNO_3: 1 (*1*), 3 (*2*) and 5 mol litre^{-1} (*3*) (author's data; unpublished).

VII. Recent results

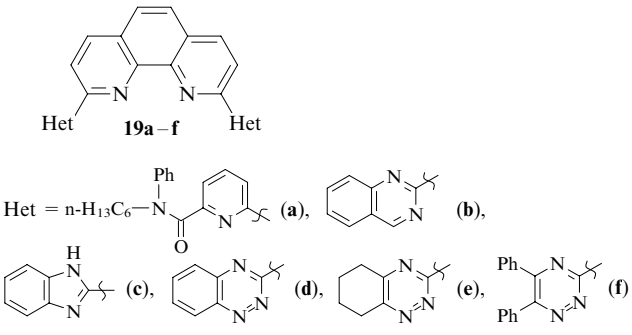
In the course of preparation of the manuscript, a number of new studies on the title topic have been published. This again emphasizes topicality of this review. We will briefly outline the most important recent results.

Researchers from India studied[112] extraction separation of actinides and lanthanides in the ionic liquids based on alkyl-methylimidazolium $[C_n mim][NTf_2]$ ($Tf = CF_3SO_2$; $n = 2–4, 6, 8$) using bis(5,6-dialkyl-1,2,4-triazinyl)pyridines whose extraction properties were considered in Section VI. Unprecedently high separation factors, $SF_{Am^{3+}/Eu^{3+}} > 3000$, obtained for the 5,6-dimethyl derivative of BTP were explained by the formation of an 1 : 4 americium complex in this system. This type of complexes was not idenitied earlier in any type of extraction systems. The results of DFT calculations[112] are indicative of higher covalency of the ligand–metal bonds for the americium complex.

Researchers from China reported[113] a combined ESI mass spectrometric and DFT investigation of the actinide and lanthanide complexes with diamide **14a** in acetonitrile. The mass spectra revealed the formation of the ($[EuL_2(NO_3)]^{2+}$) complexes at low metal : ligand ([M] : [L]) ratios and the 1 : 1 complexes at [M] : [L] $\geqslant$ 1. The results of DFT calculations were analyzed within the framework of the NBO approach and according to Bader; the molecular electrostatic potentials were also calculated. Based on the results obtained, the authors concluded that the americium–ligand bonds are more covalent than the europium–-ligand bonds.

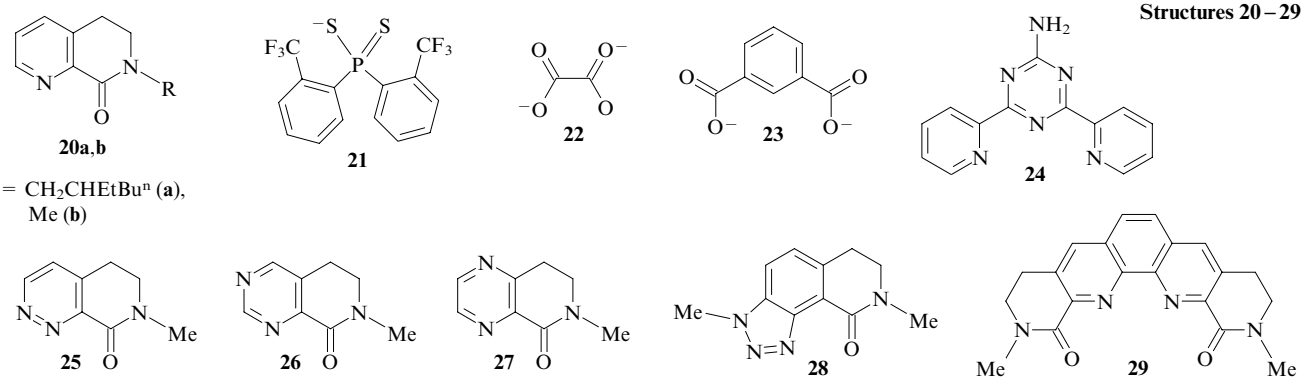
The structure, the nature of coordination bonds and the thermodynamics of the Am^{3+} and Eu^{3+} complexes with ligand **19a** containing picoline amide groups in positions 2 and 9 of the phenanthroline moiety were studied in detail by DFT calculations and analyzed using the NBO approach and according to Bader.[114] In the complexes with Am^{3+} and Eu^{3+}, compound **19a** acts as hexadentate ligand and coordinates the cations through four nitrogen atoms and the oxygen atoms of both amido groups. According to calculations, the cationic complex $[ML(NO_3)_2]^+$ is the most stable nitrate complex. Ligand **19a** is expected to be more selective for americium compared to europium in the extraction experiments.

Structures 19



In the next study[115] carried out in the same research group the selectivity of the 1,10-phenanthroline ligands **10b**

Structures 20 – 29



and **19b – d** bearing heterocyclic donor groups in positions 2 and 9 of the phenanthroline moiety for lanthanides and actinides is considered within the framework of the HSAB concept. It was shown that the softer ligands exhibit higher selectivity for actinides.

The extraction properties of three 1,10-phenanthroline ligands **19d – f** with donor heterocyclic substituents in positions 2 and 9 for lanthanides and actinides were theoretically investigated [116] using density functional B3LYP/6-31G(d)/RECP and MP2/6-31G(d)/RECP methods. According to calculations of the structures and properties of complexes of the type $[LnL_2(NO_3)]^{2+}$, the Gibbs energies of formation of the complexes decrease with increasing atomic number of the lanthanide in the order Eu, Tb, Tm; this agrees with the results obtained in other studies [109, 112] of this type of ligands.

The role of triazinyl groups in the bonding of actinides and lanthanides with 2,6-bis(triazinyl)pyridines was assessed in a computational DFT study.[117] The formation of complexes with 2,6-bis(2-pyridyl)pyridine (TPY) and 2-(2-pyridyl)-6-triazinylpyridine (hemi-BTP) was studied for comparison.

Researchers from Poland reported [118] a DFT examination of the conformations of water-soluble 2,6-bis(triazinyl)pyridines containing triazinyl groups 3-sulfophenyl substituents in positions 5 and 6 and their solvation by water molecules. For the first time, these ligands were studied using a model in which five water molecules in the first coordination sphere and the ligand molecule were considered in the supermolecule approximation. Solvation of the supermolecule was described using the PCM model. According to calculations, the most stable configurations are identical to those observed for protonated BTP ligands. Hydroxonium ions formed in solvation of the sulfo groups can migrate to the coordination cavity of the ligand and bind nitrogen atoms. Thus, the metal ion should displace the hydroxonium ion in the course of extraction. The model proposed in that study is consistent with our model [98] for the mechanism of extraction of lanthanides and actinides by pyridine-2,6-dicarboxylic acid diamides.

An excellent study by Bryantsev and Hay [119] occupies a particular position among recent publications. In order to estimate the selectivity of novel ligands containing donor O-, N- and S-centres, the authors attempted to find a well-reasoned answer to a major question formulated in Section II.1: what high-level quantum chemical methods should be used to predict the separation factors in the extraction separation of actinides and lanthanides? They examined a total of eleven different-type ligands (compounds **20a,b** and **21 – 29**) and calculated the selectivity in the extraction separation of americium and europium using different DFT methods.

Calculations were carried out using the relativistic core potentials, two GGA-functionals (BPE and BP86), the B3LYP hybrid functional, the local *meta*-GGA-functional M06-L, the hybrid *meta*-GGA-functional M06. Four different basis sets (6-31G*, 6-311G**, 6-31+G** and 6-311++G**) were tested for B3LYP and one (6-31+G**) was used for the other density functionals. The solvation effects were considered including water molecules from the first coordination sphere to a supermolecule and then solvation of the supermolecule was described using the COSMO approach. The solvents were dichloroethane, trifluoromethyl phenyl sulfone and kerosene and the chemical model was represented by the equilibrium (34).

$$[Am(H_2O)_9]^{3+}_{(aq)} + [EuL_n(NO_3)_3]_{(org)} \rightleftharpoons \rightleftharpoons [AmL_n(NO_3)_3]_{(org)} + [Eu(H_2O)_9]^{3+}_{(aq)} \quad (34)$$

On the basis of detailed analysis of the structural factors governing the selectivity in the extraction separation of actinides and lanthanides, the authors concluded: 'To allow reasonably accurate predictions, it was critical to employ sufficiently flexible basis sets and provide proper account of solvation effects'.

The results reported in the recent publications substantiate the efficiency of methods for theoretical modelling in the design of novel, highly selective ligands for the separation of actinides and lanthanides. This is the main reason for rapidly increasing number of studies on the title topic, which are carried out by research groups in different countries.

VIII. Conclusion

Although high-level quantum chemistry methods have been used for theoretical modelling of extraction separation of MA and lanthanides in processing of high-level PUREX raffinate only recently, the available results point to fruitfulness of this approach. Using these methods, a number of basic and applied problems were solved, including the following, most valuable ones.

Now researchers have a more clear idea of the nature of coordination bonds in the complexes of polydentate donor ligands with actinides and lanthanides. The results of all theoretical studies point that these bonds are mainly ionic. The covalent contribution is small. It is significantly larger

for the actinides rather than lanthanides and thus to a great extent governs the thermodynamic stability of the complexes.

By and large, the HSAB is upheld, other factors being equal. Namely, Lewis bases with softer donor N- and S-centres exhibit higher affinity for softer actinide ions. This holds for most highly selective ligands. The maximum separation factors, $SF_{An/Ln} \geqslant 10^4$, were obtained for dialkylphosphinodithioic acids. Unfortunately, these compounds are inappropriate for utilization in large-scale technologies since extraction from strongly acidic media is impossible, they have low oxidation stability and low radiation stability and form solid phosphate and sulfate residues upon ashing, which leads to cracking of matrices (see above).

The degree of involvement of the actinide and lanthanide f-AOs in the bonding is still a moot question. Based on qualitative considerations, it was assumed that the contribution of the more diffuse actinide 5f-AOs is larger than that of the lanthanide 4f-AOs. A critical analysis of the available results of calculations shows that not only nf-AOs, but also $(n+1)$p-AOs and $(n+1)$d-AOs contribute to the covalent component originating from transfer of the electron density from the bonding MOs of the ligand to the vacant AOs of the metal. In each particular case, the relative contributions of the metal AOs are determined by the nodal properties and the relative energies of the ligand MOs and the metal AOs. Complexes of actinides, in particular, uranium, are also characterized by backdonation, *i.e.*, partial transfer of the electron density from the filled metal AOs to the antibonding ligand MO of corresponding symmetry. One can accept the opinion by Dolg and coworkers [47] that the bond lengths obtained from DFT calculations of the lanthanide and actinide compounds should be used as a criterion for covalent contribution with great care because of possible uncertainties due to the 'delocalization error'.[17]

In spite of this, DFT calculations using nonempirically constructed and hybrid functionals represent the main reliable and convenient method for structure elucidation of the lanthanide and actinide complexes. The GGA-functionals (PBE, PW91, BP86) allow one to carry out computationally inexpensive calculations. Calculations with the hybrid functionals (B3LYP and PBE0) are much more time-consuming. A common and justifiable practice is to use two functionals (*e.g.*, PBE + PBE0 or BP86 + B3LYP) to validate the stability of the results obtained. In some cases, the following computational trick is used in order to make the overall procedure less labour- and time-consuming: fast calculations using a GGA-functional are followed by the energy (E and G) calculations using the GGA-optimized geometry and a hybrid density functional without additional optimization. It this case, uncertainties in the total energy values (E) can be as large as $\pm(2-5)$ kcal mol^{-1}; this should be taken into account when interpreting the results obtained.

The quality of the basis set is of paramount importance. Reliable results can be obtained using polarized split-valence basis sets augmented with diffuse functions. The inclusion of relativistic effects in the scalar-relativistic approximation or using relativistic effective core potentials allows one to obtain correct results of similar quality.

One should also take into account that fact that the potential energy surfaces of the actinide and lanthanide complexes with donor ligands of complex structure are usually characterized by a large number of local minima corresponding to different conformations with close energies. Therefore, the search for a global minimum should be carried out using different starting geometries and, when possible, without structural simpifications.

Thus, we can state with certainty that quantum chemical modelling of the structure and properties of actinide and lanthanide complexes with polydentate donor ligands is an efficient tool for solving practical problems in the extraction separation of MA and lanthanides in HLW processing in the nuclear fuel cycle and in the separation of lanthanides. Having chosen the models and computational methods properly, one can not only obtain qualitatively correct results and an explanation for the experimentally observed trends, but also use the results of calculations for prognostic purposes. The main goal of prognosis is to establish 'structure–extraction behaviour' relationships for various types of ligands, to choose the most promising ligand structures and to correctly predict the $SF_{An/Ln}$ values for particular systems. These quantities depend on a number of factors that should be taken into account.

1. The metal–ligand binding energies (ΔE and ΔG) in the complexes MLX_n are usually estimated in gas-phase calculations as the total electronic energy (E) differences and the Gibbs energy (G) differences between the fragments L and MX_n. When comparing complexes of two ligands (L^1 and L^2) or two metals (M^1 and M^2), the differences $\Delta\Delta G(ML^1X_n - ML^2X_n)$ and $\Delta\Delta G(M^1LX_n - M^2LX_n)$ can be used, other things being equal, for qualitative predictions (see, *e.g.*, Refs 65, 102, 103, 107, 109). One should keep in mind that ligand conformations in the free state and in the complex are often strongly different. High ligand 'preorganization' energies can lead to strong destabilization of the complexes. As a consequence, extraction systems should, if possible, be designed using conformationally rigid structures where the geometry of the free ligand is close to its geometry in the complex.

2. Calculations, in accordance with the available experimental data, correctly reproduce the influence of substituents in the heterocyclic moieties of ligands and at the donor centres on the binding energies. Donor substituents make the actinide and lanthanide complexes more thermodynamically stable. However, the effect of substituents on the separation factors has been studied fragmentarily as yet and deserves additional investigations.

3. The influence of anionic ligands at the metal atoms on the efficiency and selectivity of extraction has also been poorly studied. Information on the nitrate and chloride complexes and on cationic aqua complexes is available. Preliminary results of quantum chemical calculations show that anionic ligands may have strong effect on the distribution ratios and separation factors. It seems that theoretical and experimental investigations of carboxylate complexes will offer new prospects for the design of efficient extraction systems.

4. Investigations of extraction systems containing several extractants have formed an important avenue of experimental research into extraction separation of MA and lanthanides in the last decade. There is a considerable body of information on synergistic effects that are most probably due to the formation of mixed-ligand complexes containing different-type donor ligands in the inner coordination sphere of metals. This type of complexes has almost

not been studied theoretically and research in this field seems to be quite promising.

5. The formation of complexes in solutions occurs as a sequence of equilibrium processes. Therefore, the result of theoretical prognosis depends critically on how correct is the chemical model for the system under study. In particular, the fact that the complexes ML_pX_q extracted to the organic phase result from equilibrium reactions between hydrated cations $[M(H_2O)_n]^{3+}$ ($n = 8$, 9) and different-ligand neutral and charged complexes $[M(H_2O)_kX_l]^{m+}$ is of crucial importance. The hydration energies of lanthanides and actinides vary over a wide range and change regularly throughout the series and often govern the concentration ratios of all types of the species present in solution. Positions of chemical equilibria are controlled by the ΔG values, so it is these parameters that should be used to estimate the separation factors $SF_{An/Ln}$.

6. As mentioned above, assessment of solvation effects remains a stubborn problem. Electrostatic effects of the medium can be relatively easy included withn the framework of continuum models (COSMO, PCM). The available data show that these calculations can be performed using the gas-phase geometries without additional optimization. But the key role is played by the effects of specific solvation through formation of hydrogen bonds in the solute–solvent systems. Although methods for solving these problems are in principle, available, high computational cost of calculations makes them hardly applicable to real complex systems.

Summing up, the most valuable and reliable information that can be obtained at present from the results of quantum chemical modelling of the structure and properties of the actinide and lanthanide complexes with polydentate donor ligands in order to predict the extraction properties of the ligands consists in reliable establishment of qualitative trends in the changes in the separation factors in series of related compounds. This make it possible to significantly decrease the number of ligands and complexes to be synthesized and studied experimentally as compared to conventional 'reasonable screening' approach based on the intutitive and qualitative ideas and thus to reduce the expenses and to shorten the time necessary to develop novel extraction technologies for processing PUREX raffinate. Progress in this research avenue occurs very rapidly and one can expect new important results in the nearest future.

The authors of this review express their gratitude to Dr. D N Laikov and Prof. V D Kosynkin for useful discussions.

The review has been written with the financial support from the Russian Federation National Nuclear Corporation 'ROSATOM' (under Contracts 6790D signed on 16.12.2014 and 5/5974D signed on 24.11.2015) and with organizational support from the National Intellectual Development Foundation ('Innopraktika').

References

1. *Reprocessing and Recycling of Spent Nuclear Fuel* (Ed.R Taylor) (*Woodhead Publishing Series in Energy: Number 79*) (Elsevier, 2015)
2. M Yu Alyapyshev, V A Babain, Yu A Ustynyuk *Russ. Chem. Rev.* **85** 943 (2016)
3. C J Cramer *Essentials of Computational Chemistry: Theories and Models* (2nd Edn) (New York: Wiley, 2004)
4. *Computational Methods in Lanthanides and Actinides Chemistry*. (Ed. M Dolg) (Chichester; Wiley, 2015)
5. A Kovács, R J M Konings, J K Gibson, I Infante, L Gagliardi *Chem. Rev.* **115** 1725 (2015)
6. V Pershina *Russ. Chem. Rev.* **78** 1153 (2009)
7. J P Perdew, K Burke, M Ernzerhof *Phys. Rev. Lett.* **77** 3865 (1996)
8. J P Perdew, J A Chevary, S H Vosko, K A Jackson, M R Pederson, D J Singh, C Fiolhais *Phys. Rev. B* **46** 6671 (1992)
9. J P Perdew *Phys. Rev. B* **33** 8822 (1986)
10. A D Becke *Phys. Rev. A* **38** 3098 (1988)
11. J P Perdew, M Ernzerhof, K Burke *J. Chem. Phys.* **105** 9982 (1996)
12. C Adamo, V Barone *J. Chem. Phys.* **110** 6158 (1999)
13. V Vetere, B O Roos, P Maldivi, C Adamo *Chem. Phys. Lett.* **396** 452 (2004)
14. V Vetere, P Maldivi, C Adamo *J. Comput. Chem.* **24** 850 (2003)
15. Y Zhao, D G Truhlar *Acc. Chem. Res.* **41** 157 (2008)
16. J P Perdew *MRS Bull.* **38** 743 (2013)
17. A J Cohen, P Mori-Sánchez, W Yang *Chem. Rev.* **112** 289 (2012)
18. G Sshreckenbach, G A Shamov *Acc. Chem. Res.* **43** 19 (2010)
19. R J Frick, T S Hofer, A B Pribil, B R Randolf, B M Rode *J. Phys. Chem. A* **113** 12496 (2009)
20. K G Dyall *J. Chem. Phys.* **100** 2118 (1994)
21. M Dolg, X Cao *Chem. Rev.* **112** 403 (2012)
22. C J Cramer, D G Truhlar *Chem. Rev.* **99** 2161 (1999)
23. S Miertuš, E Scrocco, J Tomasi *Chem. Phys.* **55** 117 (1981)
24. R Cammi, J Tomasi *J. Comput. Chem.* **16** 1449 (1995)
25. J Andzelm, J C Kölmel, A Klamt *J. Chem. Phys.* **103** 9312 (1995)
26. B Mennucci *Comput. Mol. Sci.* **2** 386 (2012)
27. P D'Angelo, A Zitolo, V Migliorati, G Mancini, I Persson, G Chillemi *Inorg. Chem.* **48** 10239 (2009)
28. C Beuchat, D Hagberg, R Spezia, L Gagliardi *J. Phys. Chem. B* **114** 15590 (2010)
29. M Bühl, H Kabrede, R Diss, G Wipff *J. Am. Chem. Soc.* **128** 6357 (2006)
30. G A Shamov, G Schreckenbach *J. Phys. Chem. A* **109** 10961 (2005)
31. J Wiebke, A Moritz, X Cao, M Dolg *Phys. Chem. Chem. Phys.* **9** 459 (2007)
32. P D'Angelo, F Martelli, R Spezia, A Filipponi, M A Denecke *Inorg. Chem.* **52** 10318 (2013)
33. J-H Lan, W-Q Shi, L-Y Yuan, J Li, Y-L Zhao, Z-F Chai *Coord. Chem. Rev.* **256** 1406 (2012)
34. Y Zhu, J Chen, R Jiao *Solv. Extract. Ion Exchange* **14** 61 (1996)
35. G Tian, Y Zhu, J Xu *Solv. Extract. Ion Exchange* **19** 993 (2001)
36. K S Boland, D E Hobart, S A Kozimor, M M MacInnes, B L Scott *Polyhedron* **67** 540 (2014)
37. C Boheme, G Wipff *Inorg. Chem.* **38** 5734 (1999)
38. C Boheme, G Wipff *Chem.–Eur. J.* **7** 1398 (2001)
39. B Coupez, C Boheme, G Wipff *J. Phys. Chem. B* **107** 9484 (2003)
40. S Meskaldji, L Belkhiri, T Arliguie, M Fourmigué, M Ephritikhine, A Boucekkine *Inorg. Chem.* **49** 3192 (2010)

41. X Cao, D Heidelberg, J Ciupka, M Dolg *Inorg. Chem.* **49** 10307 (2010)
42. M B Jones, A J Gaunt, J C Gordon, N Kaltsoyannis, M P Neu, B L Scott *Chem. Sci.* **4** 1189 (2013)
43. A Bhattacharyya, T K Ghanty, P K Mohapatra, V K Manchanda *Inorg. Chem.* **50** 3913 (2011)
44. M D Tissandier, K A Cowen, W Y Feng, E Gundlach, M H Cohen, A D Earhart, J V Coe, T R Tuttle *J. Phys. Chem. A* **102** 7787 (1998)
45. S Goldman, L R Morss *Can. J. Chem.* **53** 2695 (1975)
46. M Dolg, X Cao, J Ciupka *J. Electron Spectrosc. Relat. Phenom.* **194** 8 (2014)
47. N Heinz, J Zhang, M Dolg *J. Chem. Theory Comput.* **10** 5593 (2014)
48. J Zhang, N Heinz, M Dolg *Inorg. Chem.* **53** 7700 (2014)
49. J M Keith, E R Batista *Inorg. Chem.* **51** 13 (2012)
50. J R Klaehn, D R Peterman, M K Harrup, R D Tillotson, T A Luther, J D Law, L M Daniels *Inorg. Chim. Acta* **361** 2522 (2008)
51. F H David, V Vokhmin *New J. Chem.* **27** 1627 (2003)
52. S A Ansari, P Pathak, P K Mohapatra, V K Manchanda *Chem. Rev.* **112** 1751 (2012)
53. C-Z Wang, J-H Lan, Q-Y Wu, Y-L Zhao, X-K Wang, Z-F Chai, W-Q Shi *Dalton Trans.* **43** 8713 (2014)
54. M R Antonio, D R McAlister, E P Horwitz *Dalton Trans.* **44** 515 (2015)
55. J Narbutt, A Wodyński, M Pecul *Dalton Trans.* **44** 2657 (2015)
56. A K Singha Deb, A Bhattacharyya, S M Ali, K T Shenoy, S K Ghosh *Sep. Sci. Techol.* **50** 395 (2015)
57. S Pahan, A Boda, S M Ali *Theor. Chem. Acc.* **134** Art. No. 41 (2015)
58. A K Singha Deb, S M Ali, K T Shenoy, S K Ghosha *Mol. Simul.* **41** 490 (2015)
59. S A Ansari, P N Pathak, M Husain, A K Prasad, V S Parmar, V K Manchanda *Radiochim. Acta* **94** 307 (2006)
60. Y Sasaki, P Rapold, M Arisaka, M Hirata, T Kimura, C Hill, G Cote *Solv. Extract. Ion Exchange* **25** 187 (2007)
61. P N Pathak, S A Ansari, S V Godbole, A R Dhobale, V K Manchanda *Spectrochim. Acta, Part A* **73** 348 (2009)
62. A E Reed, L A Curtiss, F Weinhold *Chem. Rev.* **88** 899 (1988)
63. *The Quantum Theory of Atoms in Molecules: from Solid State to DNA and Drug Design* (Eds C F Matta, R J Boyd) (Weinheim; Wiley-VCH, 2007)
64. S Kannan, M A Moody, C L Barnes, P B Duval *Inorg. Chem.* **47** 4691 (2008)
65. A K Singha Deb, B N Mohanty, P Ilaiyaraja, K Sivasubramanian, B Venkatraman *J. Radioanal. Nucl. Chem.* **295** 1161 (2013)
66. M Sundararajan, S K Ghosh *J. Phys. Chem. A* **115** 6732 (2011)
67. K Shimojo, H Naganawa, J Noro, F Kubota, M Goto *Anal. Sci.* **23** 1427 (2007)
68. A S Suneesh, K A Venkatesan, K V Syamala, M P Antony, P R Vasudeva Rao *Radiochim. Acta* **100** 425 (2012)
69. A S Suneesh, R Kumaresan, S Rajeswari, P K Nayak, K V Syamala, K A Venkatesan, M P Antony, P R Vasudeva Rao *Sep. Sci. Technol.* **48** 1998 (2013)
70. G E Persson, S Svantesson, S Wingefors, J O Liljenzin *Solv. Extract. Ion Exchange* **2** 89 (1984)
71. T S Grimes, R D Tillotson, L R Martin *Solv. Extract. Ion Exchange* **32** 378 (2014)
72. L E Roy, N J Bridges, L R Martin *Dalton Trans.* **42** 2636 (2013)
73. C Rabbe, V Mikhalko, J P Dognon *Theor. Chem. Acc.* **104** 280 (2000)
74. G Ionova, C Rabbe, R Guillaumont, S Ionov, C Madic, J-C Krupa, D Guillaneux *New J. Chem.* **26** 234 (2002)
75. D Guillaumont *J. Phys. Chem. A* **108** 6893 (2004)
76. L Petit, C Adamo, P Maldivi *Inorg. Chem.* **45** 8517 (2006)
77. L Petit, C Daul, C Adamo, P Maldivi *New J. Chem.* **31** 1738 (2007)
78. G Benay, R Schurhammer, J Desaphy, G Wipff *New J. Chem.* **35** 184 (2011)
79. J Narbutt, W P Oziminski *Dalton Trans.* **41** 14416 (2012)
80. A Bremer, C M Ruff, D Girnt, U Müllich, J Rothe, P W Roesky, P J Panak, A Karpov, T J J Müller, M A Denecke, A Geist *Inorg. Chem.* **51** 5199 (2012)
81. F W Lewis, L M Harwood, M J Hudson, M G B Drew, M Sypula, G Modolo, D Whittaker, C A Sharrad, V Videva, V Hubscher-Bruder, F Arnaud-Neu *Dalton Trans.* **41** 9209 (2012)
82. C de Sahb, L A Watson, J Nadas, B P Hay *Inorg. Chem.* **52** 10632 (2013)
83. A Zaiter, B Amine, Y Bouzidi, L Belkhiri, A Boucekkine, M Ephritikhine *Inorg. Chem.* **53** 4687 (2014)
84. Z Kolarik *Chem. Rev.* **108** 4208 (2008)
85. P J Panak, A Geist *Chem. Rev.* **113** 1199 (2013)
86. Z Szabó, T Toraishi, V Vallet, I Grenthe *Coord. Chem. Rev.* **250** 784 (2006)
87. G Y S Chan, M G B Drew, M J Hudson, N S Isaacs, P Byers, C Madic *Polyhedron* **15** 3385 (1996)
88. C Adam, P Kaden, B B Beele, U Müllich, S Trumm, A Geist, P J Panak, M A Denecke *Dalton Trans.* **42** 14068 (2013)
89. G Benay, R Schurhammer, G Wipff *Phys. Chem. Chem. Phys.* **13** 2922 (2011)
90. J-H Lan, W-Q Shi, L-Y Yuan, Y-L Zhao, J Li, Z-F Chai *Inorg. Chem.* **50** 9230 (2011)
91. J-H Lan, W-Q Shi, L-Y Yuan, Y-X Feng, Y-L Zhao, Z-F Chai *J. Phys. Chem. A* **116** 504 (2012)
92. C L Xiao, Q Y Wu, C Z Wang, Y L Zhao, Z F Chai, W Q Shi *Sci. China Chem.* **57** 1439 (2014)
93. F W Lewis, L M Harwood, M J Hudson, M G B Drew, V Hubscher-Bruder, V Videva, F Arnaud-Neu, K Stamberg, S Vyas *Inorg. Chem.* **52** 4993 (2013)
94. Y Marcus *Biophys. Chem.* **51** 111 (1994)
95. A N Carolan, G M Cockrell, N J Williams, G Zhang, D G VanDerveer, H-S Lee, R P Thummel, R D Hancock *Inorg. Chem.* **52** 15 (2013)
96. M Yu Alyapyshev, V A Babain, L I Tkachenko, I I Eliseev, A V Didenko, M L Petrov *Solv. Extract. Ion Exchange* **29** 619 (2011)
97. M Yu Alyapyshev, V A Babain, L I Tkackenko *Radiochemistry* **56** 565 (2014) [*Radiokhimiya* **56** 481 (2014)]
98. Yu A Ustynyuk, I P Gloriozov, S N Kalmykov, A A Mitrofanov, V A Babain, M Yu Alyapyshev, N A Ustynyuk *Solv. Extract. Ion Exchange* **32** 508 (2014)
99. F Renaud, C Piguet, G Bernardinelli, J-C G Bünzli, G Hopfgartner *Chem. – Eur. J.* **3** 1646 (1997)
100. F Renaud, C Piguet, G Bernardinelli, J-C G Bünzli, G Hopfgartner *Chem. – Eur. J.* **3** 1660 (1997)

101. K C Majumadar, N De, S Chakravorty *Synth. Commun.* **41** 121 (2011)
102. G V Lavrov, N A Ustynyuk, I P Gloriozov, Yu A Ustynyuk, M Yu Alyapyshev, L I Tkachenko, V A Babain, in *Sbornik Tezisov Mezhdunarodnogo Kongressa po Khimii Geterotsiklicheskikh Soedinenii 'KOST-2015'* (Abstracts of Reports of the International Congress on The Chemistry of Heterocyclic Compounds 'KOST-2015', Moscow 2015) p. 239
103. Yu A Ustynyuk, G V Lavrov, N A Ustynyuk, I P Gloriozov, M Yu Alyapyshev, L I Tkachenko, V A Babain, in *Sbornik Tezisov Konferentsii 'Radiokhimiya-2015'* (Abstracts of Reports of the Conference 'Radiochemistry-2015', Zheleznogorsk, 2015) p. 127
104. A Paulenova, M Yu Alyapyshev, V A Babain, R S Herbst, J D Law *Solv. Extract. Ion Exchange* **31** 184 (2013)
105. C-L Xiao, C-Z Wang, L-Y Yuan, B Li, H He, S Wang, Y-L Zhao, Z-F Chai, W-Q Shi *Inorg. Chem.* **53** 1712 (2014)
106. C-L Xiao, Q-Y Wu, C-Z Wang, Y-L Zhao, Z-F Chai, W-Q Shi *Inorg. Chem.* **53** 10846 (2014)
107. D Manna, S Mula, A Bhattacharyya, S Chattopadhyay, T K Ghanty *Dalton Trans.* **44** 1332 (2015)
108. D Manna, T K Ghanty *Phys. Chem. Chem. Phys.* **14** 11060 (2012)
109. Yu A Ustynyuk, N E Borisova, V A Babain, I P Gloriozov, A Y Manuilov, S N Kalmykov, M Yu Alyapyshev, L I Tkachenko, E V Kenf, N A Ustynyuk *Chem. Commun.* **51** 7466 (2015)
110. C A Chang, M E Rowland *Inorg. Chem.* **22** 3866 (1983)
111. M Alyapyshev, V Babain, N Borisova, I Eliseev, D Kirsanov, A Kostin, A Legin, M Reshetova, Z Smirnova *Polyhedron* **29** 1998 (2010)
112. A Bhattacharyya, S A Ansari, T Gadly, S K Ghosh, M Mohapatra, P K Mohapatra *Dalton Trans.* **44** 6193 (2015)
113. C-L Xiao, C-Z Wang, L Mei, X-R Zhang, N Wall, Y-L Zhao, Z-F Chai, W-Q Shi *Dalton Trans.* **44** 14376 (2015)
114. H Wu, Q-Y Wu, C-Z Wang, J-H Lan, Z-R Liu, Z-F Chai, W-Q Shi *Dalton Trans.* **44** 16737 (2015)
115. H Wu, Q-Y Wu, C-Z Wang, J-H Lan, Z-R Liu, Z-F Chai, W-Q Shi *Dalton Trans.* **45** 8107 (2016)
116. Y Yang, Y Fang, J Liu, Shi Hu, Sheng Hu, L Yang, D Wang, H Zhang, S Luo *J. Mol. Model.* **21** Art. No. 185 (2015)
117. Y-N Liang, X Yang, S Ding, S Li, F Wang, Z Chai, D Wang *New J. Chem.* **39** 7716 (2015)
118. J E Rode, J Narbutt, M K Dudek, S Kaźmierski, J Cz Dobrowolski *J. Mol. Liq.* **219** 224 (2016)
119. V S Bryantsev, B P Hay *Dalton Trans.* **44** 7935 (2015)